Global Biogeochemical Cycles

REVIEW ARTICLE
10.1029/2022GB007657

Special Section:
REgional Carbon Cycle Assessment and Processes - 2

Inland Water Greenhouse Gas Budgets for RECCAP2: 1. State-Of-The-Art of Global Scale Assessments

Ronny Lauerwald[1], George H. Allen[2], Bridget R. Deemer[3], Shaoda Liu[4,5], Taylor Maavara[4,6], Peter Raymond[4], Lewis Alcott[7], David Bastviken[8], Adam Hastie[9,10], Meredith A. Holgerson[11], Matthew S. Johnson[12], Bernhard Lehner[13], Peirong Lin[14], Alessandra Marzadri[15], Lishan Ran[16], Hanqin Tian[17], Xiao Yang[18], Yuanzhi Yao[19], and Pierre Regnier[20]

[1]Université Paris-Saclay, INRAE, AgroParisTech, UMR ECOSYS, Palaiseau, France, [2]Department of Geosciences, Virginia Polytechnic Institute and State University, Blacksburg, VA, USA, [3]U.S. Geological Survey, Southwest Biological Science Center, Flagstaff, AZ, USA, [4]Yale School of the Environment, Yale University, New Haven, CT, USA, [5]State Key Laboratory of Water Environment Simulation, School of Environment, Beijing Normal University, Beijing, China, [6]School of Geography, University of Leeds, Leeds, UK, [7]Department of Earth & Planetary Sciences, Yale University, New Haven, CT, USA, [8]Department of Thematic Studies—Environmental Change, Linköping University, Linköping, Sweden, [9]Carbon and Wetlands Group, Faculty of Science, Charles University, Prague, Czech Republic, [10]School of GeoSciences, University of Edinburgh, Edinburgh, UK, [11]Department of Ecology and Evolutionary Biology, Cornell University, Ithaca, NY, USA, [12]Earth Science Division, NASA Ames Research Center, Moffett Field, CA, USA, [13]Department of Geography, McGill University, Montreal, QC, Canada, [14]School of Earth and Space Sciences, Institute of Remote Sensing and GIS, Peking University, Beijing, China, [15]Department of Civil, Environmental and Mechanical Engineering, University of Trento, Trento, Italy, [16]Department of Geography, The University of Hong Kong, Hong Kong, China, [17]Department of Earth and Environmental Sciences, Boston College, Schiller Institute for Integrated Science and Society, Chestnut Hill, MA, USA, [18]Department of Earth Sciences, Southern Methodist University, Dallas, TX, USA, [19]School of Geographic Sciences, East China Normal University, Shanghai, China, [20]Department Geoscience, Environment & Society—BGEOSYS, Université Libre de Bruxelles, Bruxelles, Belgium

Key Points:

- We explore the state-of-the-art in inland water greenhouse gas emissions, discussing existing estimates and underlying methodologies
- Development of models increasingly allows for assessment of spatial and temporal variability of emission fluxes
- There is a persisting need for observations that capture hot-spots and hot-moments in emissions, including from small water bodies

Correspondence to:
R. Lauerwald,
ronny.lauerwald@inrae.fr

Citation:
Lauerwald, R., Allen, G. H., Deemer, B. R., Liu, S., Maavara, T., Raymond, P., et al. (2023). Inland water greenhouse gas budgets for RECCAP2: 1. State-of-the-art of global scale assessments. *Global Biogeochemical Cycles*, *37*, e2022GB007657. https://doi.org/10.1029/2022GB007657

Received 26 NOV 2022
Accepted 19 APR 2023

Author Contributions:
Conceptualization: Ronny Lauerwald, George H. Allen, Bridget R. Deemer, Peter Raymond, David Bastviken, Bernhard Lehner, Pierre Regnier
Data curation: Ronny Lauerwald, George H. Allen, Taylor Maavara, Adam Hastie, Matthew S. Johnson, Bernhard Lehner, Alessandra Marzadri, Hanqin Tian, Xiao Yang, Yuanzhi Yao
Formal analysis: Ronny Lauerwald, George H. Allen, Bridget R. Deemer, Taylor Maavara, Lewis Alcott, Meredith A. Holgerson, Matthew S. Johnson, Bernhard Lehner, Alessandra Marzadri, Xiao Yang, Yuanzhi Yao

Abstract Inland waters are important emitters of the greenhouse gasses (GHGs) carbon dioxide (CO_2), methane (CH_4), and nitrous oxide (N_2O) to the atmosphere. In the framework of the 2nd phase of the REgional Carbon Cycle Assessment and Processes (RECCAP-2) initiative, we review the state of the art in estimating inland water GHG budgets at global scale, which has substantially advanced since the first phase of RECCAP nearly 10 years ago. The development of increasingly sophisticated upscaling techniques, including statistical prediction and process-based models, allows for spatially explicit estimates that are needed for regionalized assessments of continental GHG budgets such as those established for RECCAP. A few recent estimates also resolve the seasonal and/or interannual variability in inland water GHG emissions. Nonetheless, the global-scale assessment of inland water emissions remains challenging because of limited spatial and temporal coverage of observations and persisting uncertainties in the abundance and distribution of inland water surface areas. To decrease these uncertainties, more empirical work on the contributions of hot-spots and hot-moments to overall inland water GHG emissions is particularly needed.

1. Introduction

Inland waters (streams, rivers, lakes and reservoirs) are net-sources of greenhouse gasses (GHGs) to the atmosphere. They receive considerable amounts of reactive organic matter from terrestrial ecosystems, promoting the production of GHGs like carbon dioxide (CO_2), methane (CH_4), and nitrous oxide (N_2O). Inland waters are usually net-heterotrophic, meaning CO_2 production through respiration exceeds CO_2 consumption by aquatic production (Battin et al., 2023). An additional source of inland water GHG emission comes from terrestrial and wetland runoff and drainage that can be oversaturated in dissolved CO_2 produced by microbial and root respiration (Abril & Borges, 2019). Once this supersaturated aqueous solution enters surface waters, it can release gas into the atmosphere and contribute to inland water CO_2 emissions. Similarly, inland waters receive dissolved CH_4 and N_2O from oversaturated soils and groundwater (Jurado et al., 2017; Rasilo et al., 2017). In addition, the sharp fronts between reducing and oxidizing conditions within the water column or at the interface between surface and subsurface environments (e.g., benthic and hyporheic zones) promotes the production and emissions of N_2O (Marzadri et al., 2017, 2021). Moreover, autochthonous aquatic production may enhance nitrification in the water column through increased oxygen levels, while it may stimulate denitrification and methanogenesis in reducing,

Methodology: Ronny Lauerwald, George H. Allen, Bridget R. Deemer, Lewis Alcott, David Bastviken, Adam Hastie, Meredith A. Holgerson, Bernhard Lehner, Hanqin Tian, Xiao Yang, Yuanzhi Yao, Pierre Regnier
Supervision: Ronny Lauerwald, Pierre Regnier
Validation: Ronny Lauerwald, Bridget R. Deemer, David Bastviken, Meredith A. Holgerson, Alessandra Marzadri
Visualization: Ronny Lauerwald, George H. Allen, Lewis Alcott
Writing – original draft: Ronny Lauerwald, George H. Allen, Bridget R. Deemer, Taylor Maavara, Peter Raymond, Lewis Alcott, David Bastviken, Adam Hastie, Meredith A. Holgerson, Matthew S. Johnson, Lishan Ran, Hanqin Tian, Xiao Yang, Yuanzhi Yao, Pierre Regnier
Writing – review & editing: Ronny Lauerwald, George H. Allen, Bridget R. Deemer, Taylor Maavara, Peter Raymond, Lewis Alcott, David Bastviken, Adam Hastie, Meredith A. Holgerson, Matthew S. Johnson, Peirong Lin, Alessandra Marzadri, Lishan Ran, Hanqin Tian, Xiao Yang, Yuanzhi Yao, Pierre Regnier

benthic sediments through delivery of labile organic matter. These processes play an important role in the N_2O and CH_4 budgets of eutrophic lakes and reservoirs (DelSontro et al., 2018; Zhou et al., 2021).

While the processes driving GHG production have been known to limnologists for some time, large-scale quantification of inland water GHG emissions is still difficult and estimates are afflicted by large uncertainties. In their 5th Assessment Report (AR5), the IPCC (2013) acknowledged for the first time that inland waters are a significant contributor to the global GHG budget. At the same time, however, it was recognized that GHG fluxes from these ecosystems remain poorly constrained at the global scale. High uncertainties in inland water GHG emission estimates arise due to a poor spatial and temporal coverage of direct observations (Bastviken et al., 2011; Deemer et al., 2016; Regnier et al., 2013, 2022; Soued et al., 2016) and are reflected in the large range of estimated inland water GHG fluxes reported in AR5: 0.8–1.2 Pg C yr^{-1} for CO_2, 8–73 Tg CH_4 yr^{-1} for CH_4, and 0.1–2.9 Tg N yr^{-1} for N_2O. In their 6th Assessment Report (AR6), the IPCC (2021) provides updated ranges for N_2O (0.5–1.1 Tg N yr^{-1}) and CH_4 (112–217 Tg CH_4 yr^{-1}) emissions which are narrower, but still reflect significant uncertainties in estimating inland water GHG emissions. Note that inland water emissions proportionally remain the largest source of uncertainty in the global land CH_4 budget (Canadell et al., 2011).

The REgional Carbon Cycle Assessment and Processes (RECCAP) initiative aims to establish the GHG budgets of large regions covering the entire globe at the scale of continents (or large regions) and large ocean basins, which are then synthesized at global scale. While the first phase of this initiative (RECCAP1; Canadell et al., 2011) focused on CO_2 only, now the second phase (RECCAP2) accounts for the three GHGs CO_2, CH_4, and N_2O. As part of RECCAP1, Raymond et al. (2013) re-estimated global inland water CO_2 evasion suggesting that the total flux could be as high as 2.1 Pg C yr^{-1}, which is about twice the estimates synthesized in AR5. This much higher estimate was due to a re-estimation of stream surface areas including small headwater streams which contribute disproportionately to the total water surface area and CO_2 emission, but which were neglected in earlier assessments that used data sets representing only larger global rivers (e.g., Cole et al., 2007). More importantly, Raymond et al. (2013) provided the first global maps of inland water CO_2 emissions, which allowed for the use of these estimates in regionalized, global C budgets (Bastos et al., 2020; Ciais et al., 2021; Zscheischler et al., 2017).

Since RECCAP1, a growing number of global estimates of inland water GHG emissions have been published, not only for CO_2 emissions (e.g., Holgerson & Raymond, 2016; Horgby et al., 2019; Lauerwald et al., 2015; Liu et al., 2022), but also for CH_4 (e.g., Holgerson & Raymond, 2016; Rosentreter et al., 2021; Stanley et al., 2016) and N_2O (e.g., Hu et al., 2016; Lauerwald et al., 2019; Maavara et al., 2019; Marzadri et al., 2021; Soued et al., 2016; Yao et al., 2020), or for all three GHGs combined (e.g., Deemer et al., 2016; DelSontro et al., 2018). The limited availability and quality (e.g., length and frequency of time-series), and uneven global coverage of observed emission rates (see e.g., Deemer et al., 2016) still represent a large source of uncertainty. While many studies build largely on the same data that was produced over the past decades, the amount and quality of empirical data is steadily increasing. In addition, global emission estimates profited from the appearance of new, improved data sets of inland water surface areas (Allen & Pavelsky, 2018; Lehner et al., 2011; Messager et al., 2016; Verpoorter et al., 2014). Finally, global scale estimation of inland water GHG budgets have been improved through novel upscaling techniques based on statistical (e.g., DelSontro et al., 2018; Lauerwald et al., 2015) and process-based models of varying complexity (e.g., Maavara et al., 2019; Yao et al., 2020).

In the framework of RECCAP2, we present a review of existing global estimates of inland water GHG emissions. We start with a general overview of methods to achieve global scale estimates, starting from methods to measure flux rates in the field, followed by methods used to upscale flux rates to the global scale and which comprise a large range of approaches including simple upscaling based on average observed flux rates, statistical prediction and the use of process-based models (Section 2). Then, in three subsections respectively dedicated to estimates of emissions of CO_2 (Section 3), CH_4 (Section 4) and N_2O (Section 5), we discuss the state of the art for each of these GHGs in more detail, review all existing global estimates, and explore differences between flux assessments and their underlying methods. In addition, we highlight for each GHG persisting shortcomings and challenges for future research. The companion paper in the same issue (Lauerwald et al., 2023) then builds on the present review to derive a regionalized assessment for the 10 regions used in RECCAP2. In this companion paper, each previously published global estimate reported here was rescaled using the same new global assessment of inland water surface area, allowing for better consistency and homogeneity across all previously published values.

2. Overview of Upscaling Strategies and Surface Area Estimates Used in Global Studies of Inland Water GHG Emissions

This subsection gives a brief overview of different methods that are used to obtain global scale estimates of inland water GHG emissions. These methods are classified into three main approaches, namely direct upscaling based on observations Section 2.1, statistical upscaling based on functional relationships between emissions and environmental drivers Section 2.2, and process-based models Section 2.3. We also briefly review progress in the global scale assessment of inland water surface areas Section 2.4, which is of vital importance for global upscaling of inland water GHG emissions.

2.1. Upscaling Based on Observations

Large-scale estimates of inland water GHG emission fluxes F_{GHG} are usually calculated as the product of an average flux rate f_{GHG}, which can be expressed in units of mass per area and time, as derived from a set of field observations, and an estimate of the inland water surface area A_{IW} for which this flux rate is assumed to be representative (Equation 1).

$$F_{GHG} = f_{GHG} * A_{IW} \quad (1)$$

Many estimates have applied this simple upscaling technique directly at the global scale using an average f_{GHG} multiplied by the total A_{IW} of one specific type of inland waters. For instance, Deemer et al. (2016) calculated the average rates of GHG emissions from reservoirs, using observations from empirical studies around the world and multiplied those average rates by the estimated total area of reservoirs after Lehner et al. (2011). Others have first broken down the total of inland waters of one type into different subgroups, for example, based on size of water body or stream order (Holgerson & Raymond, 2016; Humborg et al., 2010), geographic region (e.g., Aufdenkampe et al., 2011; Bastviken et al., 2011; Johnson et al., 2021; Soued et al., 2016) or both (Raymond et al., 2013; Rosentreter et al., 2021). An area-integrated flux from each subgroup was then calculated following the same Equation 1, before summing those up to a global flux.

Methods and challenges to obtain estimates of A_{IW} are presented in detail in Section 2.4. In what follows, we will first focus on uncertainties associated with measuring and calculating f_{GHG}. Flux rates can either be obtained from GHG emission rates directly measured in the field (Section 2.1.1), or from measurements or calculation of GHG concentration gradients and concomitant measurements or models of gas transfer velocities (Section 2.1.2). Note that this study does not aim to provide a detailed review of field methods. These aspects are thus only briefly discussed, with a focus on methodological uncertainties.

2.1.1. Directly Observed Flux Rates

A common method to measure aquatic GHG emission rates is the use of floating chambers, which resemble inverted plastic buckets put onto the water surface. The emission rates are then calculated based on the accumulation rate of GHGs within the floating chamber headspace. This method detects the emission rate from the small surface area of the floating chamber across the larger area over which the chamber may be moving during the deployment. Chambers may drift a few meters if tethered or over longer distances if drifting freely during the deployment (Lorke et al., 2015). Such a well-defined footprint is advantageous for studies of local flux regulation and for distinguishing variability in space versus time. Concurrently, the small size of the footprint leads to potentially high uncertainties in the extrapolation of flux chamber measurements to large areas, without numerous representative measurements (Colas et al., 2020). Eddy covariance towers, though less common and only applicable in standing water bodies of a certain size have the advantage of generating net fluxes (i.e., emission or uptake) from a larger surface area (depending on height, surface roughness and wind speeds, eddy covariance towers can have a footprint of up to 3-km radius (Chu et al., 2021)), thus delivering a more representative emission rate (Podgrajsek et al., 2014). In contrast to the floating chamber method, the eddy covariance technique also allows for continuous measurements which provide better temporal resolution in emission rates. However, the flux footprint is constantly moving with wind speed and direction, making variability in time and space challenging to distinguish (Eugster et al., 2011). Fluxes cannot be measured at all when there is no wind (e.g., typical during night time) and complications associated with rainfall and lateral advective gas flux make accurate flux measurements challenging (Podgrajsek et al., 2014; Vesala et al., 2006). Eddy covariance also relies on the performance of advanced equipment and a high level of operator expertise for adequate data filtering and

QA/QC. Above all, limited eddy covariance measurements mean that global upscaling based only on this method is not yet possible, and inherent limitations due to its vulnerability toward unfavorable meteorological conditions and interactions with other nearby ecosystems make eddy covariance suboptimal for key inland water emission measurements such as fluxes from streams and along lake shores.

While the majority of CO_2 and N_2O emissions occur through diffusive flux across the air-water interface, a significant but variable fraction of aquatic CH_4 flux occurs as bubbles (i.e., ebullition) (Bastviken et al., 2011). Ebullition occurs when CH_4 produced in aquatic sediments forms gas bubbles that at a certain size, due to buoyancy, evade the sediment layer and ascend through the water column. Existing emission estimates from floating chambers sometimes intentionally exclude ebullition (e.g., Yang et al., 2021). Other floating chamber methods include both diffusive and ebullitive emissions (e.g., Barbosa et al., 2021). Also, eddy covariance towers measure the sum of both emission pathways (Eugster et al., 2011). There are nonetheless various methods to directly quantify ebullition. However, these methods detect bubbles rather than CH_4 and need supplementary measurements of CH_4 concentration within the bubble gas, usually from manually taken samples, to allow flux estimation (e.g., Linkhorst et al., 2020). This point is critical as CH_4 concentration in bubbles can vary widely, from less than 1% to >80% (Boereboom et al., 2012). The most common methods for directly quantifying ebullition rates is the bubble trap, an inverted funnel that collects ascending bubbles (Maeck et al., 2013) and is sometimes connected to a hydrostatic pressure sensor (Varadharajan et al., 2010) or specialized bubble size sensors (Delwiche & Hemond, 2017) to measure the timing and size distribution of ascending bubbles. Ebullition measurements based on point measurements in space and time are currently very labor intensive given the high spatiotemporal variability of ebullitive fluxes (Linkhorst et al., 2020). Echo sounders (Ostrovsky et al., 2008), robotic boats connected to optical methane detectors (Grinham et al., 2011) and under-ice surveys (Wik et al., 2011) have also been used to quantify ebullition rates. In addition, radar remote sensing approaches are currently being developed that could integrate over space and time for more representative measurements (Engram et al., 2020).

2.1.2. Estimating Diffusive Fluxes Based on Concentration Gradients

The methods for directly measuring emission rates can easily be applied in deeper, slower-moving waters (floating chambers and funnel traps) or in larger water bodies (eddy covariance). However, these methods are often not feasible for smaller streams. Instead, emission flux rates can be calculated from a gradient in concentrations of a specific GHG (ΔC_{GHG}) in the water close to the surface and in the overlying atmosphere and a gas exchange velocity k_{GHG} (Equation 2). Note that this method can be applied to flowing and standing water bodies of any size, but only allows estimation of diffusive emissions, and is not applicable for ebullition. The gradient ΔC_{GHG} can be calculated based on direct field measurements using headspace equilibration methods (e.g., Müller et al., 2015), or using measured headspace partial pressures and solubility constants that depend on salinity and water temperature (Weiss, 1970).

$$f_{GHG} = \Delta C_{GHG} * k_{GHG} \quad (2)$$

The headspace equilibration method consists of equilibrating a known volume of sampled water and a known volume of air or gas, with a known initial partial pressure of the GHG to be analyzed. After full equilibration, a sample of the headspace is analyzed by for example, gas chromatography (Natchimuthu, Wallin, et al., 2017), optical gas analyzers (Grilli et al., 2020), or other gas analysis methods, to measure the corresponding GHG partial pressure from which the C_{GHG} in the sampled surface water can be calculated. This concentration is compared with the theoretical concentration in equilibrium with the background air partial pressure of the GHG in focus to yield ΔC_{GHG}. In the case of CO_2, concentrations can also be calculated from observations of alkalinity and pH based on chemical equilibria and the assumption that non-carbonate contributions to alkalinity are negligible, which can be questioned in some common aquatic systems (Abril et al., 2015) (see Section 3.2 for more discussion).

Gas exchange velocity can be assessed through direct tracer studies in which a specific tracer gas is injected into the stream, and its loss is measured over a defined length. As this method is too cumbersome and costly to be applied everywhere, empirical equations have been established that relate k_{GHG} to the rate of energy dissipation at the water-air interface. Energy dissipation causes the turbulent mixing of the upper water column and thus determines the depth of the water column which interacts with the atmosphere through the process of diffusion. In fact, k_{GHG} in units of length per time (e.g., m day^{-1}) represents the depth of the upper water column that will equilibrate with the overlying atmosphere over that specific amount of time. For streams and rivers, this

energy dissipation rate can be estimated from stream flow velocity and stream channel geometry, in particular the slope of the stream channel (Natchimuthu, Sundgren, et al., 2017; Natchimuthu, Wallin, et al., 2017; O'Connor & Dobbins, 1958; Raymond et al., 2012). More recent work has however noted a breakpoint in the energy dissipation rate at which air entrainment and bubble formation cause k_{GHG} to increase more rapidly with energy dissipation (Ulseth et al., 2019). This suggests that assuming only diffusive water-air gas exchange, as it is assumed in most studies of inland water CO_2 emissions, may lead to underestimated gas transfer velocities in systems with very high hydrological energy. For lakes and reservoirs, empirical equations relate k_{GHG} to wind speed (Cole & Caraco, 1998), lake surface area (Read et al., 2012), or both (Vachon & Prairie, 2013), as the degree to which wind shear versus convective mixing dominate gas transfer dynamics generally changes as a function of waterbody size. More sophisticated modeling of k_{GHG} from lake hydrodynamics considering multiple turbulence-generating processes have also been developed (e.g., MacIntyre et al., 2021). It has been suggested that models of k_{GHG} should be locally validated whenever possible (e.g., Schilder et al., 2013).

2.2. Upscaling Based on Statistical Prediction

A variety of statistical methods have been used to upscale flux measurements/estimates to the global scale. These methods can be categorized into two groups of statistical upscaling approaches: (a) methods that predict emission rates directly, and (b) methods that first predict A_{IW}, ΔC_{GHG}, and k_{GHG} separately, and combine them using Equations 1 and 2 to estimate the emission flux $F_{GHG,IW}$.

A simple example for the first group of methods is the use of emission factors (EFs), which has been applied to estimate N_2O emissions from river networks (Beaulieu et al., 2011; Kroeze et al., 2010). Averaged EFs, typically defined as the ratio of N_2O emissions to riverine N loads, were derived from a number of field studies. These EFs were then multiplied by global, spatially explicit estimates of river N loads (e.g., Mayorga et al., 2010) to estimate global riverine N_2O emissions at the same spatial resolution as the riverine N loads. This method assumes that riverine N_2O emissions simply scale linearly to riverine N loads, which is problematic from a reaction kinetics point of view, as discussed in Maavara et al. (2019). As an alternative empirical approach, Hu et al. (2016) used findings from field studies to fit equations predicting riverine N_2O emissions as a nonlinear function of dissolved inorganic N yield and catchment area, thus overcoming some of the limitations of the EF approach.

Another prominent example for the first group of methods is the study by DelSontro et al. (2018), predicting global lake CH_4 emissions empirically. DelSontro et al. (2018) fitted multilinear regression equations to a database of literature studies of 166 water bodies quantifying lake CH_4 emissions, that predict the total (diffusive + ebullitive), annual emission flux from lake size and lake productivity (defined as chlorophyll or phosphorus concentration). The fitted regression equations were then applied to different global data sets/estimates of lake surface area and an assumed statistical distribution of lake productivity across global lakes to estimate the global-scale CH_4 emissions from these water bodies.

Examples for the second group of methods are the studies by Raymond et al. (2013), Lauerwald et al. (2015), and Horgby et al. (2019) that estimated CO_2 emissions from rivers at the global scale or for specific ecoregions (Horgby et al., 2019 focused on alpine streams). These studies all used global data sets including digital elevation models and their derivatives (stream network and channel slope) and gridded estimates of average annual river flow to explicitly estimate stream surface area and k_{GHG} spatially. While Raymond et al. (2013) combined their estimates of A_{IW} and k_{GHG} with regionalized averages of calculated ΔC_{CO2}, Lauerwald et al. (2015) and Horgby et al. (2019) further used multiple linear regression models to estimate riverine ΔC_{CO2} from different spatial drivers (like terrestrial Net Primary Productivity—NPP, climate, terrain steepness in Lauerwald et al. (2015), or elevation, soil carbon stocks, and discharge in Horgby et al. (2019)). Note that combining independent estimates of k_{GHG} and ΔC_{GHG} introduces an additional source of uncertainty, as ΔC_{GHG} is in turn controlled by k_{GHG} and its balance with CO_2 resupply rates to the surface water, which is for instance evidenced by low ΔC_{GHG} in turbulent, high alpine streams (Horgby et al., 2019).

2.3. Process-Based Models

Process-based models of varying degrees of complexity have recently been used to assess inland water GHG emission at the global scale (Maavara et al., 2019; Marzadri et al., 2021; Yao et al., 2020). Ideally, such models represent carbon and nutrient transport and transformation processes that drive production, cycling and emission

of GHGs in a water body or along a cascade of water bodies (like a sequence of stream reaches or a cascade of reservoirs along a river network). This representation requires boundary condition data at the global scale and in sufficient quality and quantity. This data requirement is a major limitation for the applicability of process-based models for inland water GHG emissions at the global scale.

A promising strategy to overcome that limitation is the explicit representation of inland waters and associated biogeochemical processes in land surface models (LSMs) that simulate the terrestrial cycling of energy, water, C, nutrients, and GHGs. Using LSMs, the biogeochemical and transport processes that drive the GHG dynamics can be simulated simultaneously for terrestrial and freshwater ecosystems, reducing the need for complex boundary conditions at the land-inland water interface. Developments in that direction have been achieved for the LSMs DLEM (Tian, Yang, et al., 2015; Tian, Ren, et al., 2015; Yao et al., 2020) and ORCHIDEE (Lauerwald et al., 2017, 2020). At global scale, LSM simulations including inland water GHG emissions have yet only been achieved with DLEM (Yao et al., 2020).

When using LSMs, the simulated water fluxes and associated terrestrial C and nutrient inputs to inland waters are already afflicted by considerable uncertainties, including those arising from the overparameterization of these extremely complex models. Thus, an alternative is to use process-based models of only inland waters forced by data driven information. The global river network N_2O modeling studies by Maavara et al. (2019) and Marzadri et al. (2021) follow two different strategies to overcome data limitations to constrain the models. Maavara et al. (2019) followed a metamodeling strategy, for which a box model representing all major processes of N and N_2O cycling in a water body was first set-up. While this process-based model could not be applied at global scale due to data limitations to constrain each biogeochemical process, Maavara and colleagues ran the model across a realistic range of model input parameters using a Monte Carlo approach to derive simple response functions. The resulting response functions relating N_2O emissions to nutrient loads and water residence times were then applied at global scale using loads and residence times derived from available global data sets. Marzadri et al. (2021) applied their process-based model of river N_2O emissions directly at global scale, which required spatially resolved model inputs comprising a detailed set of parameters describing stream hydro-morphology and water quality, which in that form did not yet exist at global scale. To overcome that limitation, machine learning techniques were applied to derive these input data sets from other, available geodata. These input data were then used to feed a process-based model that parametrizes N_2O emissions as a function of river size by means of two Damköhler numbers representing the ratio between a characteristic time of transport and a characteristic time of reaction. The proposed hybrid model (machine learning + process based) allows the consideration of the contribution of surface (e.g., water column) and subsurface (e.g., benthic and hyporheic zones) processes to N_2O emissions (Marzadri et al., 2021).

For aquatic CH_4 emissions, process-based modeling efforts have been mostly dedicated to lake and reservoir systems. For example, an online, open-source predictive model framework "G-res" has recently been developed to provide global, spatially explicit estimates of the form and magnitude of reservoir CH_4 and CO_2 emissions (Harrison et al., 2021; Prairie et al., 2021). G-res uses a series of calibrated empirical models that integrate local (reservoir-specific) and regional (watershed attributes) information to predict GHG emissions (Prairie et al., 2021). The model has been applied to 4,727 reservoirs to estimate global emissions (Harrison et al., 2021). Tan and Zhuang (2015a, 2015b) have developed and applied a process-based model to estimate CH_4 emissions from lakes at pan-arctic scale. That model produces gridded output, resolves seasonal and interannual variability, and permits for projections of long-term trends following global change scenarios.

2.4. Available Data and Previous Estimates of Global Inland Water Surface Area

The first digital global map of inland water surface areas that was used for inland water GHG emission estimates was the Global Lake and Wetland Database (GLWD) by Lehner and Döll (2004). GLWD was derived from a compilation of different global and regional inventories. While GLWD is not globally consistent with regard to detail and reliability of the data sources, it represented the best available data set for more than a decade and was used in numerous studies of inland water GHG emissions (e.g., by Raymond et al. (2013) for lakes and reservoirs, by Aufdenkampe et al. (2011) for all water bodies). Since then, our ability to estimate the global surface area of rivers, lakes, and reservoirs has progressed significantly. This progress has been driven by advances in satellite remote sensing, image processing methods, and geospatial analysis techniques. Several freely available global hydrography data sets have recently become available that can be used to estimate surface area and distribution

of inland water bodies. Here we discuss a selection of high-resolution, freely available data sets that can be useful for global-scale evaluations of greenhouse gas emissions from inland water bodies.

A few global inland water body data sets have been developed using optical remote sensing data. The JRC GSW data sets from Pekel et al. (2016) and the GSWD from Pickens et al. (2020) are two global 30-m-resolution data sets of open surface water extent, created from the Landsat archive. These data sets are multitemporal and highly consistent but they do not distinguish between different water body types (e.g., rivers, lakes, etc.). Classifying water body type is necessary in evaluations of GHG exchange because of differing exchange rates and processes occurring in different aquatic environments. The Global River Widths from Landsat (GRWL) database (Allen & Pavelsky, 2018) contains exclusively river surface areas derived from Landsat imagery.

In addition to these image-based data sets, global topography-based data sets derived from digital elevation models (DEMs) have been used for representing the global extent and distribution of streams and rivers. These include hydrologically conditioned gridded raster data sets like HydroSHEDS (Lehner et al., 2008) and MERIT Hydro (Yamazaki et al., 2019) or vectorized flowline data sets derived from these gridded data sets including HydroRIVERS (Lehner & Grill, 2013) or MERIT Hydro–Vector (Lin et al., 2021). These DEM-based data sets can be used to infer the location and size of narrow rivers and streams too small to be visible from freely available satellite data sets. These data sets can also be used to infer other characteristics of river networks including stream order, slope, upstream area, and topology, which are of potential value for estimating amount and turbulence of river flow, which in turn are important drivers of GHG emissions. Other hydrography data sets innovatively combine DEM-based data sets with other sources of data to produce novel information including machine learning-based estimates of river surface area (Lin et al., 2021) and the extent of non-perennial rivers (Lin et al., 2021; Messager et al., 2021).

For standing open water bodies like lakes and reservoirs, attempts have also been made to identify water bodies from satellite imagery using automated algorithms. A prominent example is the Global Water Body (GLOWABO) data set (Verpoorter et al., 2014). Due to the unsupervised classification method and the fact that ground truth was evaluated only for Sweden, this data set is however uncertified for other parts of the world and likely contaminated with wrongly assigned riverine, coastal or temporal water bodies (Pi et al., 2022). In addition, inventory-based data sets have further been developed, including the Global Reservoir and Dam database (GRanD) (Lehner et al., 2011) and the HydroLAKES database (Messager et al., 2016) which gives water surface areas of standing waters distinguishing lakes from reservoirs. Note that HydroLAKES also includes the information from GRanD and GLWD, which makes these products partly redundant. The advantage of inventory-based data sets as GRanD and HydroLAKES is the avoidance of contamination with other water bodies and additional attributes such as names, estimates of water volume and residence time, height and purpose of dam for reservoirs, etc. In particular the distinction between lakes and reservoirs is of major importance for the assessment of inland water GHG emissions. Reservoirs as artificial water bodies deserve special attention, as they represent an anthropogenic source of GHGs and a potential lever for controlling future emissions (Almeida et al., 2019). However, we have to expect an under-classification of reservoirs in inventory data sets such as HydroLAKES, as water bodies for which this information was not available have been categorized as natural lakes by default (Messager et al., 2016). Smaller hydropower projects which outnumber large hydropower projects by approximately 11:1 (Couto & Olden, 2018) may not always be inventoried and accounted for in regional and global data sets. Recently, new data sets of dams and reservoirs have been created combining remote sensing-based data sets with other sources of information, for example, GOODD (Mulligan et al., 2020) and GeoDAR (Wang et al., 2021), continuously increasing the numbers of reservoirs that are taken up into inventories.

Although considerable progress has been made recently in developing global hydrography data sets, much less work has been done to apply these data sets to estimate global surface area of inland water bodies. For the surface area of rivers, three notable global estimates have been produced by Downing et al. (2012) of between 485,000 and 682,000 km^2, Raymond et al. (2013) of between 487,000 and 761,000 km^2, and Allen and Pavelsky (2018) of 773,000 $\pm$ 79,000 km^2. Downing et al. (2012) based their estimate on >400 observations of stream width, data on number and length of streams from HydroSHEDS data set, and statistical scaling relating stream number, width and length to stream order. While this observational data set covers rivers from all over the world, it is clearly dominated by North American rivers and the extent to which the statistical relationships identified in that study is applicable to the global-scale is questionable. Raymond et al. (2013) combined the stream network of HydroSHEDS with gridded runoff data to obtain a distribution of stream lengths and discharge per stream order

of medium to large rivers, to which they then applied empirical, hydraulic equations predicting stream width from discharge. Finally, they used stream-order based scaling laws to estimate stream surface areas for smaller streams. Allen and Pavelsky (2018) used their remote-sensing based GRWL database for surface areas of medium to large rivers, which they complemented with topography- and statistical-based estimates for streams narrower than 90 m to headwater streams as defined by Allen et al. (2018). The GRWL data set is to date the most complete and reliable data set of its kind.

For the surface area of lakes and reservoirs, three notable global estimates have been made by Downing et al. (2006), Verpoorter et al. (2014), and Messager et al. (2016). Downing et al. (2006) used surface areas from standing water bodies >10 km^2 from GLWD (Lehner & Döll, 2004) and extrapolated the surface area to smaller water bodies down to 0.001 km^2 assuming power-law relationships (Pareto distributions) between water body size and frequency. Note, however, that a more recent empirical study disproved the hypothesis that number and area of small lakes would follow a power-law distribution (Cael & Seekell, 2016). Verpoorter et al. (2014) used their remote-sensing derived GloWaBo database which includes lakes as small as 0.002 km^2. Messager et al. (2016) derived their estimate from their inventory based HydroLAKES database, which contains water bodies >0.1 km^2. Due to this restriction with regard to minimum lake size, Messager et al. (2016) obtained the lowest of the three global surface area estimates for standing waters with 2.7×10^6 km^2. The estimate of Downing et al. (2006) is substantially higher with 4.2×10^6 km^2, while for water bodies larger than 0.1 km^2, their estimate of 2.9×10^6 km^2 is quite comparable to HydroLAKES. The estimate by Verpoorter et al. (2014) is even higher with 5×10^6 km^2, likely due in part to overestimation of lake areas through contamination with other water bodies (Pi et al., 2022). A reliable map of smaller bodies of standing water, such as ponds, which are thought to contribute substantially to the total water surface area and disproportionally to GHG emissions (Holgerson & Raymond, 2016; Rosentreter et al., 2021), is still not achievable.

3. Inland Water CO_2 Budget

3.1. Overview of Existing Estimates

Global estimates for the aquatic CO_2 emission range from 0.84 to 7.33 Pg CO_2 yr^{-1} for streams and rivers, from 0.40 to 2.14 Pg CO_2 yr^{-1} for lakes, from 0.08 to 0.14 Pg CO_2 yr^{-1} for reservoirs (excluding the estimate by Cole et al. (2007), which is discussed at the end of this section), and from 0.89 to 2.35 Pg CO_2 yr^{-1} for estimates that lumped lakes and reservoirs together (Table 1, Figure 1). In general, considerable discrepancies exist in particular between early estimates that relied mostly on lumped estimates of average CO_2 concentrations, k_{GHG} and water surface area, and more recent estimates relying on more complete concentration data sets, more sophisticated upscaling approaches and spatially resolved water surface area estimates. For streams and rivers, the earliest estimates (Cole & Caraco, 2001; Cole et al., 2007, p. 207) were crude and most likely underestimate riverine CO_2 emissions because of their reliance on data from large rivers, which tend to show lower areal CO_2 emission rates than smaller and more upstream systems, as large rivers tend to be less heterotrophic, receive less important inputs of CO_2 enriched groundwater, and show less turbulent stream flow which leads to lower gas exchange velocities (Raymond et al., 2013). Relying on an extensive database for pCO_2, new scaling laws for k_{GHG} and stream hydraulic geometry that allowed for spatially resolved estimates for stream surface areas at the global scale, Raymond et al. (2013) presented the first spatially explicit estimate for the aquatic CO_2 flux and reports a river CO_2 evasion rate that is 3–8 times higher than the earlier lumped estimates (Aufdenkampe et al., 2011; Cole et al., 2007; Tranvik et al., 2009). Moreover, they demonstrated the importance of small headwaters which contribute disproportionately to the total emission flux. Problematic in that approach was that average pCO_2 and k_{GHG} values, from which the fluxes were calculated, were estimated independently from each other. pCO_2 values were taken as average over large regions independent of stream order, while k_{GHG} was estimated per region and stream order with values systematically increasing toward the small stream orders. That bears the risk, in particular for low order streams, that high estimates of k_{GHG} are combined with high estimates of pCO_2, leading to unrealistic high flux rates, whereas empirical studies have shown that under higher k_{GHG} values pCO_2 normally tends to be close to equilibrium with the atmosphere (Rocher-Ros et al., 2019). More recent advancements in stream and river CO_2 evasion estimates involve the development of data-driven statistical models to resolve temporal and finer spatial scale variations of the riverine CO_2 flux (Lauerwald et al., 2015; Liu et al., 2022). For instance, relying on direct C_{CO2} measurements and seasonally varying estimates for k_{GHG} and river surface area, Liu et al. (2022) demonstrated CO_2 emission from global streams and rivers varied between 411 and 766 Tg CO_2 yr^{-1} per month, that is, by a factor of ~2, with the highest global emissions during northern summer in July.

Table 1
Global Estimates of Inland Water CO_2 Emissions

References	$\Sigma CO_{2\,em}/\Sigma A_{water}$ (g CO_2 m^{-2} yr^{-1})	ΣA_{water} (10^6 km^2)	$\Sigma CO_{2\,em}$ (Pg CO_2 yr^{-1})	Method
Rivers				
DLEM Tian, Ren, et al. (2015)	3,531	0.64	2.24	Model
Liu et al. (2022)[a]	9,900	0.672	7.33 ± 0.73[b]	Machine learning
Lauerwald et al. (2015)[a]	3,895	0.55–0.67	2.38 (1.77–3.10)[c]	Statistical prediction
Raymond et al. (2013)[a]	10,644	0.62	6.6 (5.7–7.5)[c]	Upscaling from observations + Statistical prediction
Aufdenkampe et al. (2011)	5,009	0.31–0.51	2.05	Lumped estimate
Tranvik et al. (2009)			2.02	Literature review
Cole et al. (2007)	1,492	0.74	0.84	Literature review
Streams and small rivers				
Liu et al. (2022)[a]	23,962	0.202	4.84	Machine learning
Marx et al. (2017)			3.41	Literature review
Lauerwald et al. (2015)[a]	5,842	0.14–0.26	1.16 (0.78–1.61)[c]	Statistical prediction
Mountain streams				
Horgby et al. (2019)	17,490	0.035	0.61	Statistical prediction
Large rivers				
Liu et al. (2022)[a]	4,946	0.47	2.31	Machine learning
Lauerwald et al. (2015)[a]	2,975	0.41	1.22 (0.96–1.54)[c]	Statistical prediction
Lakes and reservoirs				
DelSontro et al. (2018)	414	3.23–5.36	1.99–3.30	Avg. rates
-"-	416	4.42	1.84 (1.72–1.98)[c]	Statistical prediction
-"-	360	5.36	1.93 (1.80–2.06)[c]	Statistical prediction
-"-	276	3.23	0.89 (0.83–0.96)[c]	Statistical prediction
Raymond et al. (2013)[a]	392	3	1.17 (0.22–3.08)[c]	Avg. pCO_2 + Statistical prediction
Aufdenkampe et al. (2011)	638	2.80–4.54	2.35	Avg. rates
Lakes (including lakes with dams)				
DLEM Tian, Ren, et al. (2015)	312	2.4	0.77	Model
Holgerson and Raymond (2016)	348	5.98	2.14	Avg. rates
Tranvik et al. (2009)			1.94	Literature review
Cole et al. (2007)	257	2	0.4	Literature review
Reservoirs				
DLEM Tian, Ren, et al. (2015)	312	0.27	0.08	Model
Deemer et al. (2016)	451	0.3	0.14 (0.12–0.16)[c]	Avg. rates
Cole et al. (2007)	686	1.5	1.03	Literature review

Note. For each Estimate, the Total Water Surface Area (ΣA_{water}), the Total CO_2 Emission Elux ($\Sigma CO_{2\,em}$) and the Area Weighted Average Emission Rate ($\Sigma CO_{2\,em}/\Sigma A_{water}$) are Reported. Mass units refer to CO_2. For conversion to units of mass of C, divide by 3.67.

[a]Estimate accounts for effects of seasonal ice cover. [b]Standard error. [c]Lower and upper 90% (Deemer et al., 2016; Lauerwald et al., 2015; Raymond et al., 2013) or 95% (DelSontro et al., 2018) CI.

A process-based model has also been developed (DLEM, Tian, Ren, et al., 2015), which predicts a much lower emission rate than recent data-driven approaches (2.24 vs. 6.60–7.33 Pg CO_2 yr^{-1}) (Table 1). The DLEM estimate is however close to the estimate by Lauerwald et al. (2015) (2.38 Pg CO_2 yr^{-1}) that only accounted for emissions from medium-sized to large rivers (i.e., 3rd order and above). The large discrepancy (i.e., 2.24

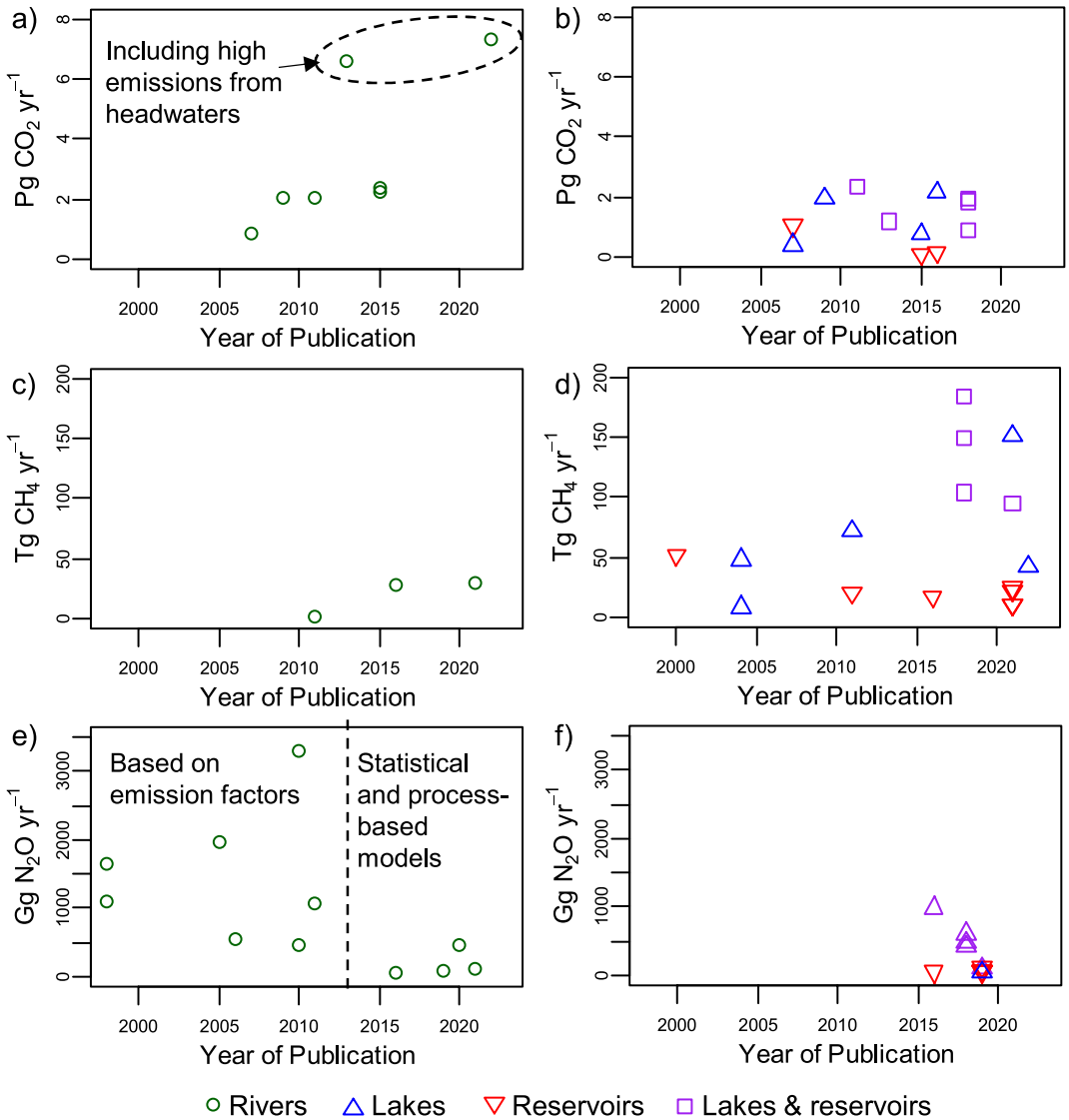

Figure 1. Estimates of inland water GHG emissions by year of publication. For rivers (a, c, e) versus Lakes and reservoirs (b, d, f), and for CO_2 (a, b), CH_4 (c, d), and N_2O (e, f).

vs. 6.60–7.33 Pg CO_2 yr^{-1}) however argues for the importance of the smallest streams in global CO_2 emission from fluvial networks (Marx et al., 2017). In line with this, Liu et al. (2022) estimated emission from the medium-to-large rivers (corresponding roughly to stream order 3 and above as in Lauerwald et al. (2015)) of ~2.31 Pg CO_2 yr^{-1}, while roughly two thirds of the total riverine emissions (~5 Pg CO_2 yr^{-1}) are predicted to be emitted by smaller streams (extrapolated to a minimum stream width of 0.3 m).

For lakes, there is a much larger variation in estimates of water surface area than in average emission rates between different studies (Table 1). In particular, estimates that relied on earlier global lake inventories (Raymond et al., 2013) report lower surface area and total emissions than more recent estimates based on newer lake inventories and extrapolated surface area to account for the smallest water bodies (DelSontro et al., 2018; Hastie et al., 2018; Holgerson & Raymond, 2016). Despite employment of scaling laws (e.g., with lake size and nutrient status) that account for spatial variability due to system size and autotrophic productivity in more recent estimates (DelSontro et al., 2018; Holgerson & Raymond, 2016; Raymond et al., 2013), there seems to be only small difference with regard to global average lake CO_2 emission rates per water surface area between those newer estimates (348–414 g CO_2 m^{-2} yr^{-1}) and those of the early crude estimates (257 g CO_2 m^{-2} yr^{-1}, Cole et al., 2007). Additionally, though earlier estimates relied more on C_{CO2} calculated from pH and alkalinity

(Cole et al., 2007; Raymond et al., 2013), more recent estimates used more often direct measurements (Delsontro et al., 2018; Holgerson & Raymond 2016). Differences in lake CO_2 evasion estimates are more driven by variation in estimates of lake area than by areal emission rates. Estimates of global average emission rates per water surface area for lakes and reservoirs (392–638 g CO_2 m^{-2} yr^{-1}) are about one order of magnitude lower than those for streams and rivers (1,492–10,644 g CO_2 m^{-2} yr^{-1}, Table 1). In comparison to lakes, reported global average emission rates per water surface area for reservoirs are slightly higher (312–686 vs. 257–348 g CO_2 m^{-2} yr^{-1} for reservoirs and lakes, respectively) (Table 1). This may in part be due to the different geographic distribution of both types of standing water bodies; with lakes being particularly abundant in high latitudes where average emission rates tend to be lower (Aufdenkampe et al., 2011). Nonetheless, the current estimates place total CO_2 evasion from reservoirs more than one order of magnitude lower than that from lakes (see Table 1, when excluding the estimate by Cole et al. (2007)), following its low share in the global surface area of standing water bodies. However, the inventory for global reservoirs (which is growing) is far from complete and thus surface area might pose the largest uncertainty for CO_2 evasion from reservoirs. Note that Cole et al. (2007), based on data from St. Louis et al. (2000), estimated a reservoir CO_2 emission of 1.03 Pg CO_2 yr^{-1}, that is, about one order of magnitude higher than the other estimates listed in Table 1. This number is based on a first-order estimate of the total surface area of reservoirs including smallest systems such as farm ponds. This estimated total area is about 5 times larger than that of reservoirs accounted for in recent inventories. While this first order estimate is an eye-opener for the underestimate related to the exclusion of these small systems, it is also highly uncertain and represents an expert opinion rather than a reproducible number. Note further that Cole et al. (2007) estimated a much lower CO_2 evasion rate from lakes, for which they rely on a much more conservative estimate of surface area which excludes smaller systems. In that regard, their emission estimate for standing waters is not consistent. Note finally that other estimates of CO_2 emissions from reservoirs might be underestimated, as in inventories, where the required information is missing, reservoirs might wrongly have been classified as lakes (see discussion in Section 2.4).

3.2. Persisting Shortcomings and Future Challenges

3.2.1. Process Understanding

In the following we discuss our current process understanding of inland water CO_2 emissions in the light of global scale estimates. Figure 2 gives an overview of the main fluxes and processes involved, while Table 2 summarizes the known effects of the major environmental drivers. The most prominent gap in the understanding of the processes that drive inland water CO_2 emissions is the question of where the emitted CO_2 is sourced from. A part of the emitted CO_2 may be produced in situ from the oxidation of allochthonous organic carbon, while another part might stem from inflows of water supersaturated in CO_2 produced during respiration in upland soils and wetlands. Further, this respiration comprises both heterotrophic respiration of plant and soil organic matter as well as autotrophic root respiration. Knowledge about the source of the aquatic CO_2 emissions is of paramount importance for the integration of these fluxes in the overall C budget of continents, as highlighted in the perspective article by Abril and Borges (2019). While earlier studies assumed that the net-CO_2 emissions are entirely the product of heterotrophic respiration and could thus be regarded as a fraction of terrestrial net-primary production (Richey et al., 2002), the contributions of autotrophic root respiration demand consideration of these fluxes as part of total ecosystem respiration that counterbalances gross primary production (Abril & Borges, 2019; Lauerwald et al., 2020).

For streams and rivers, it is assumed that most of the emitted CO_2 is sourced from CO_2 produced by respiration in adjacent wetlands, but also in upland soils, from where the CO_2 is then transported with percolating soil water and groundwater flows (Abril et al., 2014; Liu et al., 2022). The relative importance of groundwater CO_2 inputs are highest in headwaters and decrease downstream (Finlay, 2003; Horgby et al., 2019; Hotchkiss et al., 2015; Liu et al., 2022; Marx et al., 2017), while wetland inputs may be more important in lower reaches as shown for the Congo River (Borges et al., 2019). Moreover, it was shown that due to the very high oversaturation of emerging groundwater, a large part of the emission already takes place over a few hundred meters downstream of the freshwater source (Johnson et al., 2008). It would thus be required to monitor smallest headwaters directly to well capture those hot spots of aquatic CO_2 emission, for which however monitoring data are not available in sufficient quantity (Marx et al., 2017). Assessment of groundwater CO_2 inputs to inland waters would further require knowledge about groundwater C content and residence time (to quantify the outflows) for which data are limited

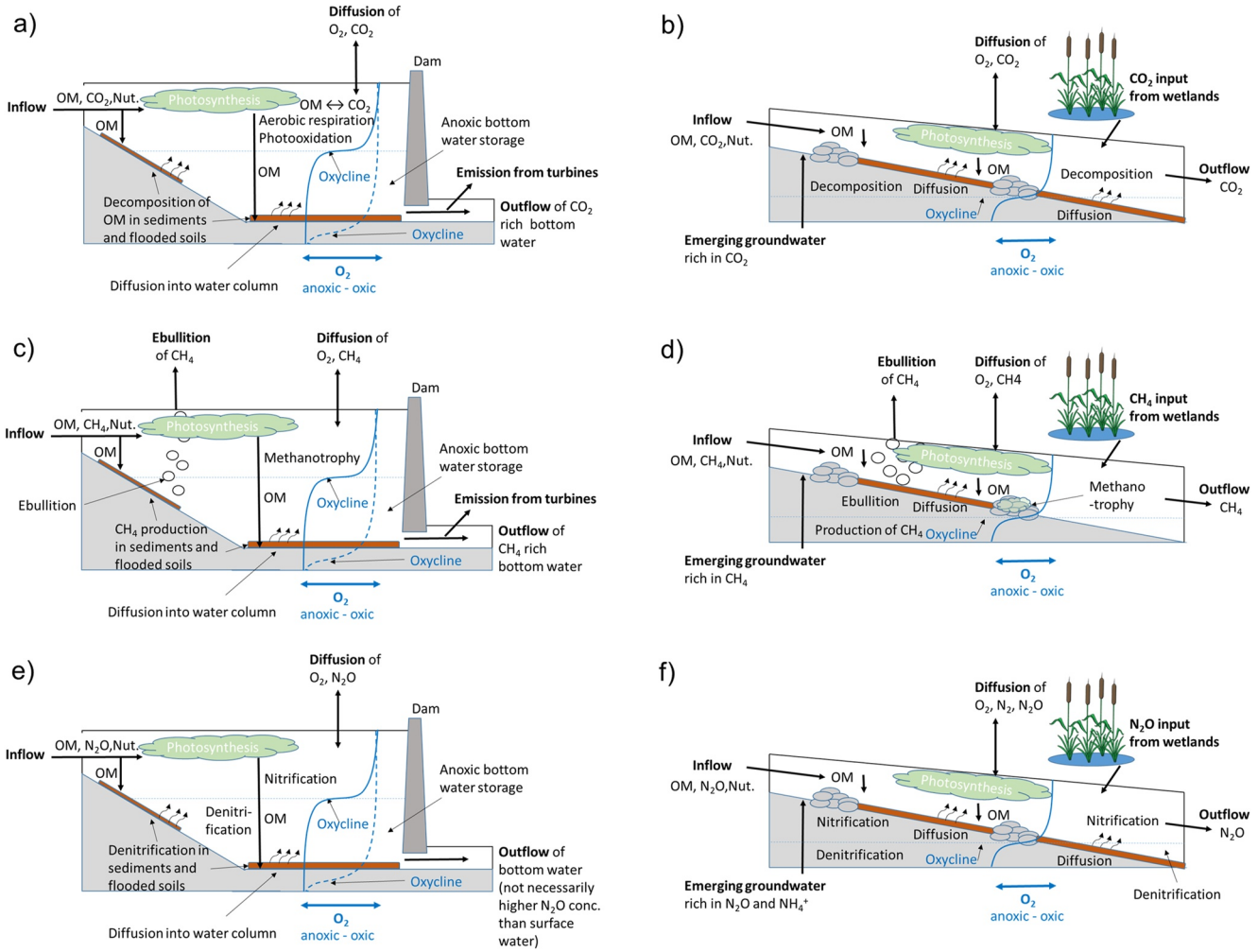

Figure 2. Schematic representation of inland water GHG budgets: for reservoirs as an example of standing waters (a, c, e) and streams/rivers (b, d, f), and for the three GHGs CO_2 (a, b), CH_4 (c, d), and N_2O (e, f). OM = organic matter; Nut. = nutrients.

as well (Downing & Striegl, 2018). While stable C isotopes have been used to estimate source contribution of riverine C loads and CO_2 emissions for single aquatic systems (Telmer & Veizer, 1999), observational data are not yet sufficient for large-scale assessment. Also, these studies do not often include the uppermost parts of the river network where large amounts of external CO_2 inputs are evading to the atmosphere.

In addition, only few existing studies of freshwater CO_2 emissions (e.g., Bogard & DelGiorgio, 2016; Crawford, Lottig, et al., 2014) have attempted to include estimates of aquatic net ecosystem production (NEP), which is the difference between aquatic production and respiration. Most studies currently assess inland waters net-CO_2 emissions rather as a black box that is fed by allochthonous C inputs. The recent study by Battin et al. (2023) has nevertheless demonstrated that the inclusion of NEP estimates can help to disentangle autochthonous CO_2 production from allochthonous CO_2 inputs even at global scale. This study corroborates the assumption that most of the aquatic CO_2 evasion is derived from external CO_2 inputs. However, also availability of aquatic NEP data is limited and does not allow yet for spatially explicit estimates at global scale. More importantly, diurnal variations in NEP may entail a similar variation in pCO_2 and air-water CO_2 exchange. Moreover, predominant sampling during daytime, when CO_2 emissions are lower than at night, may lead to important biases in flux estimations. Gómez-Gener et al. (2021) recently argued that global estimates based on daytime measurements are biased as night time emissions are on average ~30% higher.

To better understand temporal variability and potential "hot-moments" of inland water CO_2 emissions, more process understanding would be required with regard to CO_2 cycling during periods of ice-cover, spring ice-melt,

Table 2
Drivers of GHG Emissions From Different Types of Inland Waters[a]

	CO_2	CH_4	N_2O
Streams and rivers	++ GW[b] inputs	++ GW inputs	++ GW inputs
	++ Inputs from wetlands	++ Inputs from wetlands	++ Inputs from wetlands
	++ Dam outflows	++ Dam outflows	0/- Dam outflows
	+ Allochtonous OM[c]	0/+ Allochtonous OM	+ Allochtonous OM
	+ Temperature	+ Temperature	+ Temperature
	+ Discharge	? Discharge	+ Discharge
	+ O_2	-- O_2	? O_2
	+ Seasonal drying	+ Seasonal drying	0 Seasonal drying
Lakes	+ Allochtonous OM	+ Allochthonous OM	+ Allochthonous OM
	- Productivity	++ Productivity	+ Productivity
	- Depth and Surface Area	-- Depth and Surface Area	++ Nitrogen load
	+ Temperature	++ Temperature	? Depth and Surface Area
	+ O_2	-- O_2	+ Temperature
			? O_2
Reservoirs	As lakes, plus ++ OM in flooded soils	As lakes, plus ++ OM in flooded soils	As lakes, plus ++ OM in flooded soils
	+ Turbine degassing	++ Turbine degassing	0 Turbine degassing
	+ Drawdown areas	? Drawdown areas	0 Drawdown areas

Note. ++, Strong increasing effect; + Increasing effect; 0, No net-effect; -, Decreasing effect; ? Unknown or ambiguous effect.
[a]Meaning of effects. [b]GW = groundwater. [c]OM, organic matter.

spring freshet, lake-turnover, and extreme events like floods for which observations are generally rare. Only one of the studies included in our synthesis actually accounts for seasonality (Liu et al., 2022), while the other studies completely ignore seasonality in hydrodynamics, including spring freshet. Further, the estimates of lake and reservoir CO_2 emissions synthesized in our study do not account for contributions during lake-turnover, when emission rates are thought to be highest in boreal to Arctic systems (Sepulveda-Jauregui et al., 2015). Intense emissions have also been reported for periods of ice melt, during which observations are usually rare (Denfeld et al., 2018).

Raymond et al. (2013) account for intermittent drying of streams and rivers by decreasing the annual emission flux relative to the no-flow period. However, existing studies showed that during dry periods, exposed beds might show even higher CO_2 emission rates than from the water surface when inundated (Keller et al., 2020). Marcé et al. (2019) even suggest that taking into account seasonal dry falling and rewetting of bed sediments, estimates of global inland water CO_2 emissions would need to be corrected upward by at least 10%. For reservoirs specifically, existing emission estimates might even be ∼50% higher if emissions from dry falling drawdown areas were taken into account (Keller et al., 2021). On the other hand, no estimate of CO_2 emissions from occasionally or seasonally inundated floodplains are available at the global scale. More systematic investigations of flux rates from both temporally dry falling inland water beds and temporally inundated floodplains would help to refine estimates of inland water CO_2 budgets and to better integrate them into continual CO_2 budgets while avoiding gaps and overlaps with terrestrial and wetland ecosystems.

Though some studies (Deemer et al., 2016; DelSontro et al., 2018; Raymond et al., 2013) have linked CO_2 variability in lakes and reservoirs to predictors such as waterbody size, mean annual precipitation, and ecosystem productivity, the controls on within-system CO_2 spatial and temporal variations are not well understood and effective scaling relationships are still in need to better represent CO_2 evasion from lakes and reservoirs. Further, characterizations of spatial variability within water bodies are rather scarce, and the representativeness of the sampling site within an aquatic system is a large source of uncertainty (Colas et al., 2020). Finally, our estimates of reservoir CO_2 emissions do not account for fluxes from hydroelectric turbines and dam outlets, where deep, hypolimnetic water enriched in CO_2 is released (Figure 2a). River reaches directly downstream of dams have been

reported to show increased pCO_2 while this excess CO_2 is being emitted rapidly over a few tenths of river-km (Calamita et al., 2021; Guérin et al., 2006; Teodoru et al., 2015). However, more systematic observations from these parts of the inland water network are needed to quantify this source of CO_2 flux at global scale, and to complete the assessment of reservoir CO_2 emissions.

3.2.2. Spatial and Temporal Resolution

Spatially and temporally resolved estimates of inland water GHG emissions at global scale can help to better understand the role of these fluxes in the overall GHG budget, to include these fluxes in regional budgets, and to evaluate them directly against observations. The realization of spatially and temporally resolved estimates is, however, limited by the availability of observations and using the utilized estimation techniques. For rivers, global empirical, spatially explicit estimates have already been achieved at several different resolutions, specifically, 231 regions (Raymond et al., 2013), gridded at 0.5° (Lauerwald et al., 2015), and for individual river reaches (Horgby et al., 2019; Liu et al., 2022). For lakes and reservoirs, the regionalized estimate based on 231 regions by Raymond et al. (2013) is the only existing spatially explicit estimate of CO_2 emissions at the global scale. Hastie et al. (2018) achieved a spatially explicit, pan-boreal estimate of lake and reservoir CO_2 emissions at 0.5° resolution. As the only process-based model approach at global scale, spatially explicit simulations with the land surface model DLEM have been achieved at 0.5° resolution for rivers and reservoirs (Tian, Ren, et al., 2015). ORCHILEAK—the inland water branch of the land surface model ORCHIDEE has so far only been applied at the continental scale of Europe (Gommet et al., 2022) and in few large-scale basins across the world (Bowring et al., 2020; Hastie et al., 2021; Lauerwald et al., 2020).

With regard to temporal resolution, most of the empirical studies published so far represent climatologies of average annual fluxes, often without precise specification of the time frame covered by the observations (Regnier et al., 2022). The only exception at global scale is the study by Liu et al. (2022) which presents a climatology of average monthly emission fluxes from rivers, thus representing the typical seasonal cycle of riverine emissions. The process-based model DLEM simulates time-series of riverine and reservoir CO_2 emission which reflect both seasonal and interannual variability. In general, a physically based model approach appears to be the most promising strategy to obtain seasonal and interannual variations in response to climate variability, for present day but also for scenario-dependent future projections (Hastie et al., 2021; Lauerwald et al., 2020; Tian, Ren, et al., 2015).

While empirical studies have highlighted the importance of diurnal variation in water-air CO_2 exchange, temporal variations at this time-scale are not yet possible to include in estimates. Process-based models like DLEM (Tian, Ren, et al., 2015) or ORCHILEAK (Lauerwald et al., 2017) represent aquatic CO_2 emissions as net-emissions driven by allochthonous inputs of CO_2 and net-instream respiration. A simulation of the diurnal variations would however require the representation of autochthonous aquatic production, which is not yet possible.

3.2.3. Data Requirements

As for all GHGs, data required to improve inland water CO_2 emission estimates include in the first place direct observation of emission rates. Many earlier estimates relied heavily on partial pressures of CO_2 (pCO_2) calculated from pH and alkalinity (Lauerwald et al., 2015; Raymond et al., 2013), which has been demonstrated to be a significant source of error leading to an overestimation of pCO_2 particularly in freshwaters with low buffer capacity against acidification (Abril et al., 2015; Golub et al., 2017; Hunt et al., 2011; Liu et al., 2020). Liu et al. (2022), relied on direct pCO_2 observations and suggested that average pCO_2 in global streams and rivers obtained by Raymond et al. (2013) is 30% too high.

However, as alkalinity and pH are easier to measure, a vast amount of data is available from a large number of studies and in data sets from environmental agencies, with greater spatial and temporal coverage (Hartmann et al., 2014) than that of direct observation. Nevertheless, as potential biases are hard to correct at large scales, a clear preference should be given to directly observed pCO_2 values. Liu et al. (2022) synthesized 5,910 direct pCO_2 observations from 63 studies, which represents about the latest inventory of available data for stream and river systems at global scale. Delsontro et al. (2018) synthesized literature data for 7,824 lakes and reservoirs. The number of direct pCO_2 observations is still limited, but steadily growing.

Likely for logistical reasons, most observations are from developed countries which contribute most to the research of inland water GHG budgets. For this reason, systems from temperate climate regions are better represented than

tropical or high-latitude systems in remote areas (e.g., compare Deemer et al., 2016; Liu et al., 2022). However, it is these remote areas that play a potentially important role, considering the extensive lake areas in Boreal to Arctic regions, and the large river systems of the humid tropics. There has been notable progress in sampling tropical (Africa (Borges et al., 2015, 2019), Amazon (Abril et al., 2014), and SE Asia (Wit et al., 2015)) and high latitude systems (Siberia (Karlsson et al., 2021; Serikova et al., 2019), Alaska: (Sepulveda-Jauregui et al., 2015)). Despite these advancements, more observations from these poorly monitored areas would help to improve estimates of global inland water CO_2 emissions.

Further, small water bodies require more attention in sampling campaigns. Holgerson and Raymond (2016) have highlighted the potentially important contribution of small lakes and ponds to global inland water CO_2 emissions. However, a regionalized estimate was not yet possible as observations of emission rates are still scarce, and more importantly, as no spatially explicit data set yet exists that would represent such small water bodies. Datasets that present the smallest water bodies (<1 km^2) reliably would help to better integrate these important CO_2 sources into regionalized, global estimates.

Finally, increasing the number, variety and representativeness of investigated systems is only one step to reduce uncertainties in large-scale estimates of inland water CO_2 emissions. Temporal and small-scale spatial variations with small stream networks (Natchimuthu, Sundgren, et al., 2017; Natchimuthu, Wallin, et al., 2017) and with lakes (Natchimuthu, Sundgren, et al., 2017; Natchimuthu, Wallin, et al., 2017) and reservoirs (Colas et al., 2020) are substantial, and the choice of one or few sampling locations and a limited measurement period lead to large uncertainties and may introduce biases in the flux estimate for the whole waterbody. Improved investigation of CO_2 budgets of single systems requires measurements at various locations within a stream network or water body. Further, for reservoirs, observations of turbine emissions and of the release of CO_2 rich bottom waters from dams are required to better constrain these important emission pathways that are often ignored in large-scale assessments. In addition, the observations should be taken over a time period long enough to assess seasonal and inter-annual variability, and at a high enough frequency to assess short-term variations, including diurnal variations. In particular, data sets covering longer time periods such as those assembled for the US (Jones et al., 2003), China (Ran et al., 2021) and the boreal biome (Lapierre et al., 2013) are crucially needed to evaluate the extent to which trends simulated by LSMs are realistic (Regnier et al., 2022). The development and deployment of automated data loggers is a promising strategy for achieving this objective (Bastviken et al., 2015).

4. Inland Water CH_4 Budget

4.1. Overview of Existing Estimates

Global estimates of aquatic CH_4 emission range from 1.5 to 30 Tg CH_4 yr^{-1} for streams and rivers, from 8 to 151 Tg CH_4 yr^{-1} for lakes, from 9.8 to 52 Tg CH_4 yr^{-1} for reservoirs, and from 16 to 331 Tg CH_4 yr^{-1} for estimates that lumped lakes and reservoirs together (Table 3, Figure 1). The range in these emission estimates is generally more dramatic than for either CO_2 or N_2O (see Sections 3 and 5, respectively), with the exception of global CO_2 emission estimates from rivers and streams.

Some of the variation in global CH_4 emission estimates is due to large differences in the waterbody surface areas applied. For example, the earliest estimate of CH_4 emissions from reservoirs used a very rough estimate of surface area, multiplying the surface area of reservoirs in the *World Register of Dams* by a factor of four under the assumption that this would better represent the total surface area including small reservoirs and farm ponds not included in that register (St. Louis et al., 2000). This approach resulted in a surface area that is approximately three times larger than any subsequent estimate. Conversely, the earliest estimate from streams and rivers was conservative in that it applied a surface area for larger rivers only (quantifiable from global maps as the GLWD; Bastviken et al., 2011), resulting in approximately a factor of two reduction compared to subsequent estimates that also account for smaller rivers and streams. While most global estimates have ignored ice cover, Johnson et al. (2021) produced an estimate of reservoir emissions that accounted for this effect and which resulted in a CH_4 emission of 10 Tg CH_4 yr^{-1} that is half or less of any previous assessment. Harrison et al. (2021) incorporated ice cover correction into their global reservoir emission estimate, resulting in similarly low emissions from reservoir surfaces (9.8 Tg CH_4 yr^{-1}), but still yielded a higher total flux due to the inclusion of reservoir turbine degassing (22 Tg CH_4 yr^{-1}). Rosentreter et al. (2021) also incorporated an ice cover correction into their assessment of global river (30 Tg CH_4 yr^{-1}), lake (151 Tg CH_4 yr^{-1}), and reservoir (24 Tg CH_4 yr^{-1}) emissions

Table 3
Existing Global Estimates of Lake, Reservoir, and River CH_4 Flux

References	$\Sigma CH_{4em}/\Sigma A_{water}$ (g CH_4 m^{-2} yr^{-1})	ΣA_{water} (10^6 km^2)	$\Sigma CH_{4\,em}$ (Tg CH_4 yr^{-1})	Method
Rivers				
Bastviken et al. (2011)	4	0.36	1.5	Avg. rates
Stanley et al. (2016)	41.4[a]	0.65	27[a]	Avg. rates
Rosentreter et al. (2021)	66.5	0.77	30	Avg. rates
Lakes and Reservoirs				
DelSontro et al. (2018)	61.7	3.23–5.36	199–331	Avg. rates
-"-	33.7	4.42	149 (95–236)[b]	Statistical prediction
-"-	34.5	5.36	185 (119–295)[b]	Statistical prediction
-"-	32.2	3.23	104 (67–165)[b]	Statistical prediction
Holgerson and Raymond (2016)	2.7[a]	5.98	16[a]	Avg. rates
Stavert et al. (2022)	32.4	2.93	95	Statistical prediction
Lakes (including lakes with dams)				
Bastviken et al. (2004)	0.12–122.9	2.8	8–48	Avg. rates
Bastviken et al. (2011)	19.2	3.7	72	Avg. rates
Rosentreter et al. (2021)[c]	54.1	3.71–5.69	151	Avg. rates
Johnson et al. (2022)[c]	15	2.8	42 ± 18[d]	Model
Reservoirs				
St. Louis et al. (2000)	35	1.5[c]	52	Avg. rates
Bastviken et al. (2011)	40.1	0.5	20	Avg. rates
Deemer et al. (2016)	58.5	0.31	17 (12–30)[b]	Avg. rates
Rosentreter et al. (2021)[c]	63.8	0.26–0.58	24	Avg. rates
Harrison et al. (2021)[c]	28.3(62.9)[e]	0.35	9.8 (22)[e]	Model
Johnson et al. (2021)[c]	33.3	0.3	10	Model

Note. For each estimate, the total water surface area (ΣA_{water}), the total CH_4 emission flux ($\Sigma CH_{4\,em}$) and the area weighted average emission rate ($\Sigma CH_{4\,em}/\Sigma A_{water}$) are reported.

[a]Only diffusive emissions. [b]Lower and upper 90% (Deemer et al., 2016) or 95% (DelSontro et al., 2018) CI. [c]Estimate accounts for effects of seasonal ice cover. [d]Standard error. [e]Includes emissions from turbines.

(estimates upscaled from mean emission rates), but in addition also an ice melt overturn correction that reduced the impact of ice cover. Moreover, their corrections did not result in a substantial lowering of the global flux due to increases in the magnitude of areal emission rates applied. The mean areal emission rates applied to upscaling efforts vary by approximately 2, 3, and 10-fold for reservoirs, lakes, and rivers respectively. In general, there is a temporal trend wherein older data sets have lower average areal emission rates than newer data sets. Part of this trend is due to the treatment of ebullition measurements in older emission estimates. Some global estimates summarized diffusive-only estimates of methane emission (Holgerson & Raymond, 2016; Stanley et al., 2016) while others combined diffusive only areal fluxes with ebullitive + diffusive estimates without differentiating one from the other (St. Louis et al., 2000). More recent estimates (Johnson et al., 2021, 2022; Rosentreter et al., 2021) only included studies that estimated both ebullition and diffusion together. Increasing average areal emission estimates may also be due to the increased likelihood of sampling right-skewed data as sample size for water bodies increases (see Wik et al., 2016). For example, a recent data set of lake and reservoir CH_4 emissions contains some of the highest mean areal fluxes, with about 65% of the estimates contained therein published since 2015 (Rosentreter et al., 2021).

Variation in binned areal emissions (e.g., by latitude, size, and chlorophyll-a) are even larger. For example, Rosentreter et al. (2021) reported an average areal CH_4 flux from the smallest lakes (<0.001 km^2) that is nearly an order of magnitude higher than from lakes in the 0.1–1 km^2 size category, making these smallest systems responsible for 38% of the total lake CH_4 emissions (Rosenteter et al., 2021; Table 3). In addition, Bastviken et al. (2011)

reported areal reservoir CH_4 emissions from tropical regions that are an order of magnitude larger than in boreal regions (Bastviken et al., 2011), although follow-up work suggests that this discrepancy may have more to do with a lack of boreal ebullition estimates (Deemer et al., 2016) and the fact that latitude is only a weak predictor for reservoir CH_4 emission (Deemer & Holgerson, 2021; Johnson et al., 2021). Conversely, Rosentreter et al. (2021) report average areal CH_4 emissions from rivers that varied by a factor of about four by latitudinal bin, with the subtropical region (10–25° absolute latitude) producing the highest areal emissions and the temperate region (25–40° absolute latitude) producing the lowest areal emissions (Rosentreter et al., 2021).

While a variety of upscaling methods have been used to estimate inland water CH_4 emission, there does not appear to be any directional bias in the resulting estimates, that is one type of approach does not seem to systematically produce higher or lower emissions than other approaches. Many early estimates and some more recent estimates have applied the simplest empirical upscaling wherein a single areal flux was applied to a global surface area of lakes and/or reservoirs (Deemer et al., 2016; DelSontro et al., 2018; St. Louis et al., 2000), and rivers (Stanley et al., 2016). Other estimates have binned lakes and reservoirs CH_4 fluxes based on latitude (Bastviken et al., 2011), waterbody surface area (Bastviken et al., 2004; Holgerson & Raymond, 2016), primary productivity (e.g., chlorophyll a concentration; DelSontro et al., 2018), or has used some combination of these approaches (Rosentreter et al., 2021). For rivers, binning has so far only been based on latitude (Bastviken et al., 2011; Rosentreter et al., 2021). Finally, the most recent efforts to model lake and reservoir CH_4 flux have used a gridded approach that considers a variety of factors likely to influence the spatial variations in CH_4 emission including temperature, nutrients, and latitudinal variation in emission factors (Harrison et al., 2021; Johnson et al., 2021; Stavert et al., 2022).

4.2. Persisting Shortcomings and Future Challenges

4.2.1. Process Understanding

In the following we discuss our current process understanding of inland water CH_4 emissions in the light of global scale estimates. Figure 2 gives an overview of the main fluxes and processes involved, while Table 2 summarizes the known effects of the major environmental drivers. Significant progress has been made toward describing the drivers of lake and reservoir CH_4 flux, which may help improve our understanding of the spatial and temporal variability in emissions in the future. Specifically, small, shallow, productive, and low latitude lakes and reservoirs have been found to show higher areal methane emissions than larger, deeper, less productive, high latitude systems (Deemer & Holgerson, 2021). In northern systems, methane emissions are often further binned by lake type, with yedoma, peat, and glacial lakes exhibiting different patterns and magnitudes of emission (Kuhn et al., 2021; Matthews et al., 2020; Wik et al., 2016). Ebullition is usually reported to be the major emission path with flux rates nearly one order of magnitude higher than that of diffusion on average (Bastviken et al., 2011), though being less important in deeper parts of standing water bodies (>12 m depth in the study by Grinham et al. (2011)). CH_4 emissions from turbines and from anoxic hypolimnic water released from dams have been shown to be important emission paths (Delwiche et al., 2022; Harrison et al., 2021; Teodoru et al., 2015), but are still ignored in most global scale assessments. Less is known about the key drivers of river CH_4 flux. Two of the three existing global estimates of river and stream CH_4 flux use latitude to bin emissions, but the latitudinal trend does not appear to describe much of the spatial variability (Rosentreter et al., 2021). The earlier data set compiled by Stanley and others contained many estimates from anthropogenically impacted rivers and streams (Stanley et al., 2016), and could be one explanation for the high global emission estimate despite only considering diffusive fluxes. While for many stream and river systems, CH_4 emissions seem indeed to be dominated by the diffusive path (Rovelli et al., 2022), ebullition has been reported to contribute substantially to stream CH_4 emissions at least locally (Crawford, Lottig, et al., 2014; Rovelli et al., 2022). Further, the effect of nutrient enrichment and productivity on river methane emissions has not been established the way it has been for lake and reservoir CH_4 emissions (Beaulieu et al., 2019). And even for lakes and reservoirs, empirical evidence for this connection between productivity and CH_4 emissions is limited ($R^2 = 0.38$ in Beaulieu et al., 2019).

Temperature is generally considered an important predictor of aquatic CH_4 emission and relationships between temperature and CH_4 flux have been used to scale seasonal emissions from reservoirs (Harrison et al., 2021; Johnson et al., 2021; Prairie et al., 2021). Such temperature-corrections address biases in many flux observations where measurements are focused during the spring-to-fall period whereas lower emissions during the ice-free winter period are typically not recorded. Temperature is considered a main driver of CH_4 production (Yvon-Durocher

et al., 2014), which limits both ebullitive and diffusive emissions. It was however found that ebullition responds much more intensely to temperature, in particular with regard to long-term trends. In a series of mesocosm experiments around the Northern Hemisphere, Aben et al. (2017) found that an increase in temperature by 4°C led to 51% higher annual ebullitive emissions, while diffusive emissions did not seem to be affected. While there is compelling cross-ecosystem evidence of increasing CH_4 emission with increasing temperature (Yvon-Durocher et al., 2014) there are also examples of systems where CH_4 oxidation is able to keep pace or surpass CH_4 production at higher temperatures (Duc et al., 2010; Shelley et al., 2015). A recent synthesis of CH_4 oxidation in lakes and reservoirs showed that CH_4 oxidation efficiency declines with ecosystem productivity (e.g., trophic status, D'Ambrosio & Harrison, 2021). In contrast, other studies have shown an increase in CH_4 oxidation with productivity (Grasset et al., 2020). Similarly, Sawakuchi et al. (2021) showed experimental evidence that CH_4 oxidation may be phosphorus-limited in northern lakes, also providing further evidence of more complex interactions between lake CH_4 dynamics and nutrient levels. The synergetic effects of productivity and temperature as driving factors of CH_4 emissions, and in particular ebullition as dominant emission path, have been shown in experimental studies (Davidson et al., 2015, 2018). Future work could improve our process understanding of methane emission dynamics by disentangling the role of temperature and productivity in driving both total emission and the balance between methane production and consumption.

Within a single waterbody, CH_4 emissions generally vary substantially in space and time (Wik et al., 2016), and this variation is likely more substantial than for either CO_2 or N_2O. This spatial and temporal variability has been shown to cause bias in upscaling, where too few measurements in either space or time can lead to underestimation of fluxes (Wik et al., 2016). While the regionalization exercise carried out in our companion paper (Lauerwald et al., 2023) begins to address seasonality by applying an ice cover and ice melt correction, future work should aim to better constrain temporal variability in methane fluxes within single water bodies. Temporal variability can arise from seasonal dynamics such as ice melt (Denfeld et al., 2018), fall turnover (Mayr et al., 2020), seasonal water-level changes (Varadharajan et al., 2010), or in response to phytoplankton blooms (Waldo et al., 2021). Diel variation can also be important. Daytime sampling might overestimate CH_4 flux in lakes (Sieczko et al., 2020), but may underestimate it in wetlands (Anthony & MacIntyre, 2016; Godwin et al., 2013; Poindexter et al., 2016). Episodic events can also be the source of large temporal variation such as water level drops in reservoirs (Harrison et al., 2017), storm-driven drops in hydrostatic pressure (Mattson & Likens, 1990) or increases in wind shear stress (Joyce & Jewell, 2003). In connection to seasonal or occasional water level drops, it was found that dry falling bed sediments tend to emit CH_4 at lower rates than when inundated, but are still a stronger source than upland soils (Paranaiba et al., 2022). For rivers, elevated discharge can lead to higher methane fluxes, especially in small high-gradient streams where methane is sourced predominantly from groundwater (Natchimuthu, Sundgren, et al., 2017; Natchimuthu, Wallin, et al., 2017). Spatial variability in aquatic CH_4 fluxes can arise for both biological and physical reasons. In lakes and reservoirs, the main drivers are the spatial variability of sedimentation of allochthonous and autochthonous organic matter (Maeck et al., 2013) and the reactivity of the sediment organic matter (Sobek et al., 2012; Wilkinson et al., 2015). Accordingly, higher fluxes are observed in inlets (DelSontro et al., 2011), near the shores (Natchimuthu et al., 2016; Peixoto et al., 2015) and behind run-of-river dams (Maeck et al., 2013). Further, spatial variability in CH_4 fluxes may arise from the heterogeneity of the sediment matrix and associated seeps (Walter Anthony & Anthony, 2013). In rivers, physical features such as waterfalls can be particularly important sites for CH_4 emissions (Natchimuthu, Sundgren, et al., 2017; Natchimuthu, Wallin, et al., 2017). At larger scales, high gradient headwater streams comprising <1% of catchment stream surface area can contribute 30% of catchment emissions, emphasizing the need to sample throughout a catchment rather than attempting to capture network-wide flux via single measurements at river mouths (Natchimuthu, Wallin, et al., 2017).

4.2.2. Spatial and Temporal Resolution

At global scale, gridded estimates of inland water CH_4 emissions exist for reservoirs (Johnson et al., 2021), lakes (Johnson et al., 2022) and lakes and reservoirs (Stavert et al., 2022). For rivers, disaggregating global fluxes over broad latitudinal zones (Bastviken et al., 2011; Rosentreter et al., 2021) still seems to be the best possible practice. Most existing global estimates for lakes and rivers represent climatologies of annual fluxes that do not resolve the seasonal and interannual variability, and longer-term trends. Using a relatively simple, process-based model, Johnson et al. (2021, 2022) were able to represent the seasonality in lake and reservoir CH_4 emission forced by temperature and ice-cover as drivers. Long-term trends in lake CH_4 emissions due to climate change have been predicted for the hol-arctic/boreal region using a more complex process-based model (Tan &

Zhuang, 2015a, 2015b). Other complex, process-based models of lake CH_4 cycling have been developed (e.g., Lake 2.0, Stepanenko et al., 2016), but have not been applied at large-scales. A recent study has hinted at the potential of exploiting global lake physical models to estimate changes in lake CH_4 cycling (Jansen et al., 2022). Combining simulated lake temperature profiles with an empirical equation linking sediment CH_4 production rates and temperature (Yvon-Durocher et al., 2014), Jansen et al. (2022) predicted relative increases in CH_4 production rates around the globe. In contrast to CO_2 and N_2O, no efforts to model river CH_4 emissions at regional to global scales have been published yet, which may partly be due to the relative small role of rivers in inland water CH_4 emissions as well as to the complexity of processes involved and the scarcity of data for model calibration and evaluation.

4.2.3. Data Requirements

One critical uncertainty for the inland water CH_4 budget is the inability to resolve the location and total surface area of the smallest lakes and impoundments. Waterbodies <0.001 km^2 have been recently estimated to comprise 37% of the lentic methane flux (Rosentreter et al., 2021). Along the same lines, Grinham et al. (2018) have estimated for Australia that CH_4 emissions from impoundments <0.1 km^2 equal about 10% of the national land use, land use change and forestry sector emissions. Given high variability in areal emissions from these smallest water bodies it is also important to increase effort in sampling these systems to reduce uncertainty. In addition to very small lakes and impoundments, sampling effort should be increased for large lakes (>1 km^2) (Deemer & Holgerson, 2021). Given the additional importance of depth and productivity in regulating lentic CH_4 flux, spatially resolved information about the depth, chlorophyll *a*, and oxygen concentrations as well as quality and quantity of deposited organic matter in lakes and reservoirs will also help improve regional and global budgets (and overall upscaling efforts). More generally, systematic, long-term monitoring programs are needed which account for the high spatio-temporal variability in areal emission rates, in particular for ebullition, to better constrain the emissions even for individual, monitored systems. Long time-series of observations may finally help to better constrain the evolution of CH_4 production and emission in response to environmental change and climate extremes like droughts and heatwaves. This need for more and better observational data can hardly be satisfied with conventional methods, but would require the deployment of automatized observation systems and the use of remote sensing data, for which more research and development is needed. For reservoirs, finally, more observations of CH_4 emissions from turbines and of downstream release of CH_4 rich waters from dams are required to better constrain these important emission pathways, and to better assess the full impact of river daming on the CH_4 budget.

For rivers, many estimates of CH_4 emission rely on pairing concentration data with estimates of gas transfer (k_{GHG}) especially in low order streams (see Section 2.1 for further discussion). These low order systems have been observed to contribute disproportionately to CH_4 emissions at the catchment network scale despite very low CH_4 concentrations (Natchimuthu, Sundgren, et al., 2017; Natchimuthu, Wallin, et al., 2017), highlighting the need to constrain local values of k_{GHG} and/or perfect a universal physical model. Further, while most observations of stream CH_4 emissions concentrate on the diffusive pathway, ebullitive emissions can be important locally in small streams (Crawford, Stanley, et al., 2014). The development and application of empirical methods to directly measure the total GHG flux from low order streams would help constrain emissions from these systems.

5. Inland Water N_2O Budget

5.1. Overview of Existing Estimates

N_2O emissions from inland waters are poorly constrained at the global scale, which is visible in the largely divergent global estimates listed in Table 4 and shown in Figure 1: 0.05–3.3 Tg N_2O yr^{-1} for streams and rivers and 0.1–0.6 Tg N_2O yr^{-1} for lakes and reservoirs. Most existing global estimates of riverine N_2O emissions are based on modeled N loads from watersheds and emission factors (EFs), in stark contrast to CO_2 and CH_4 global estimates, which are calculated mainly by empirically upscaling local observations. N_2O is produced as an intermediate product in denitrification, that is, the reduction of nitrate to N_2, but also as a by-product in the process of nitrification, that is, the oxidation of ammonium to nitrate (Canfield et al., 2010). The amount of N_2O produced and emitted due to these processes depends on environmental and hydrological factors including water temperature, N availability and speciation, water body depth, oxygen availability, pH, and labile carbon concentrations (Clough et al., 2007; Hu et al., 2019; Outram & Hiscock, 2012; Rosamond et al., 2012; Venkiteswaran

Table 4
Global Scale Estimates of Inland Water N_2O Emissions

References	$\Sigma N_2O_{em}/\Sigma A_{water}$ (mg N_2O m^{-2} yr^{-1})	ΣA_{water} (10^6 km^2)	ΣN_2O_{em} (Gg N_2O yr^{-1})	Method
Rivers				
Seitzinger and Kroeze (1998) and Seitzinger et al. (2000)			1,650 (300–2,940)[c]	Emission factors
Kroeze et al. (2005)			1,975	Emission factors
Mosier et al. (1998)			1,100	Emission factors
De Klein et al. (2006)			550	Emission factors
Kroeze et al. (2010)			470–3,300	Emission factors
Beaulieu et al. (2011)			1,070	Emission factors
Hu et al. (2016)			51 (19–105)[a]	Statistical prediction
Maavara et al. (2019)			72–78[c]	Model
Yao et al. (2020)			458 ± 92[b]	Model
", stream orders 1–3			387 ± 93[b]	Model
", stream orders ≥4			71 ± 23[b]	Model
Marzadri et al. (2021)			114	Machine learning + Model
", stream orders 1–3			76	Machine learning + Model
", stream orders ≥4			38	Machine learning + Model
Lakes and reservoirs				
DelSontro et al. (2018)	78	3.23–5.36	252–424	Avg. rates
DelSontro et al. (2018)	106	4.42	470 (300–710)[a]	Statistical prediction
DelSontro et al. (2018)	112	5.36	600 (380–860)[a]	Statistical prediction
DelSontro et al. (2018)	127	3.23	410 (250–600)[a]	Statistical prediction
Soued et al. (2016)	235	4.20	985 ± 465[b]	Avg. rates
Lauerwald et al. (2019)	34	2.93	98 ± 64[c]	Model
Lakes (including lakes with dams)				
Lauerwald et al. (2019)	17	2.68	46 ± 29[c]	Model
Reservoirs				
Deemer et al. (2016)	152	0.31	47 (31–110)[a]	Avg. rates
Maavara et al. (2019)	148–250[c]	0.45	67–112[c]	Model
Lauerwald et al. (2019)	185	0.25	52 ± 33[c]	Model

Note. For each estimate, the total water surface area (ΣA_{water}), the total N_2O emission flux (ΣN_2O_{em}) and the area weighted average emission rate ($\Sigma N_2O_{em}/\Sigma A_{water}$) are reported.
[a]Lower and upper 90% (Deemer et al., 2016; Lauerwald et al., 2015; Raymond et al., 2013) or 95% (DelSontro et al., 2018) CI. [b]Standard error. [c]Min and max estimate.

et al., 2014). EFs can be defined as average ratios of N_2O emission to denitrification and nitrification fluxes. However, it is difficult to quantify nitrification and denitrification fluxes for entire river systems, and even more so at the global scale. Therefore, EFs have traditionally been established by linking N_2O emissions directly to riverine N loads, implicitly assuming a certain fraction of riverine N loads to be nitrified and denitrified. Mosier et al. (1998) assumed that N leached to the river network was denitrified once and nitrified twice along the river network. Further assuming that 0.25% of both nitrified and denitrified N is emitted as N_2O, they concluded that 0.75% of the total N leached to the river is emitted as N_2O. Applying that percentage as EF directly to riverine N loads, they estimated a global riverine N_2O emission of 1.1 Tg N_2O yr^{-1}. The methodology and EFs established by Mosier et al. (1998) also served to assess the river N_2O emissions in the 5th Assessment Report of the IPCC (2013).

In a similar approach, Seitzinger and Kroeze (1998) and Seitzinger et al. (2000) estimated N_2O emissions from only the dissolved inorganic fraction (nitrate, nitrite and ammonium) of N (DIN) leached to rivers. Applying

EFs of 0.3% and 3% relative to riverine DIN load they estimated a global riverine N_2O emission of 1.7 (range 0.3–2.9) Tg N_2O/yr. Over the following decade, these two EF approaches, that is, the one of Seitzinger and Kroeze (1998) and the IPCC approach derived from Mosier et al. (1998), were updated, yielding consistently large emission fluxes. Kroeze et al. (2005) estimated 2 Tg N_2O/yr, and later Kroeze et al. (2010) revised their estimate to 0.5–3.3 Tg N_2O/yr, both using modeled DIN loads and EFs of 0.3% and 3%. De Klein et al. (2006) predicted a global riverine N_2O emission of 0.6 Tg N_2O/yr, while Beaulieu et al. (2011) calculated an emission flux of 1.1 Tg N_2O/yr, both using the IPCC approach.

Studies conducted over the last 5–7 years (Hu et al., 2016; Maavara et al., 2019; Marzadri et al., 2021; Yao et al., 2020) consistently calculate N_2O emissions for rivers that are substantially lower than those of the decades before (Figure 1). Hu et al. (2016)'s empirical approach estimated global riverine N_2O emissions of 51 (19–105) Gg N_2O/yr. Further, the authors report EFs relative to riverine DIN loads of 0.16%–0.19% to be realistic, suggesting the EFs used by Seitzinger and Kroeze (1998) to be unrealistically high. Maavara et al. (2019)'s spatially resolved stochastic-mechanistic river-continuum model is the first to explicitly represent N transformation processes, and results agreed well with Hu et al.'s predictions, with a global flux of 72–78 Gg N_2O/yr. Moreover, Maavara et al. (2019) estimated that only 7% and 9% of the total N loads are respectively denitrified and nitrified in the global river network. Thus, the assumption behind the IPCC AR5 approach that all N leached to rivers is once denitrified and twice nitrified also appears to be unrealistic and responsible for gross overestimations.

The studies by Yao et al. (2020) and Marzadri et al. (2021) are complementary as they provide estimates that also account for small streams that contribute disproportionately to the overall riverine N_2O emissions, but which were ignored in earlier estimates. Marzadri et al. (2021), using a machine learning based approach, reach an estimate of about 114 Gg N_2O yr^{-1}, of which about half is contributed by headwater streams. Note that this is only a near-global estimate which excludes high latitudes >60° N, which can however be assumed to be small contributors to the global emission due to low N loads of the corresponding river systems (Maavara et al., 2019). Yao et al. (2020), using the land surface model DLEM, estimate riverine N_2O emissions at even higher values of 458 ± 92 Gg $N_2O\,yr^{-1}$, of which 80% stems from small stream emissions up to stream order 3. In their simulations, emissions from these small streams are largely fed by N_2O inputs from groundwater and saturated soils, which are not accounted for in the other studies. Marzadri et al. (2021), although not representing groundwater N_2O inputs, still estimate that about ⅔ of total riverine N_2O emissions is contributed by small streams of orders 3 and lower (see Table 4). In these small streams, nitrification-denitrification processes occur mainly within hyporheic and benthic zones, whereas in larger rivers, the contribution of water column exceeds that of subsurface environments in contributing to N_2O production (Marzadri et al., 2021). The estimates for larger rivers only by Yao et al. (2020) and Marzadri et al. (2021) agree better with those by Hu et al. (2016) and Maavara et al. (2019).

For lakes and reservoirs, the first global estimates were only published recently. Soued et al. (2016) and DelSontro et al. (2018) gave estimates for the entirety of lakes and reservoirs, without distinguishing between both types of systems while Deemer et al. (2016) estimated N_2O emission from reservoirs only. Maavara et al. (2019), in their stochastic-mechanistic model of N_2O emissions from river networks, included explicit emission estimates for reservoirs. Lauerwald et al. (2019) then adapted that model to estimate N_2O emission from both reservoirs and lakes. Soued et al. (2016) performed a simple upscaling based on averaged observed N_2O emissions rates for three latitudinal zones, which yielded with 985 ± 465 Gg N_2O yr^{-1} the highest of the emission fluxes from lakes and reservoirs listed in Table 4. A major limitation of this study was the poor global coverage of observations. While they used data from 298 systems worldwide, they had observations from only six systems for their low latitude estimate, all belonging to the reservoir-class from the study of Guérin et al. (2006). This fact is critical as in their upscaling, lakes and reservoirs from that zone contributed about 80% of their global estimate of N_2O emissions. Moreover, some of these reservoirs showed extremely high emission rates due to the fact that soils and biomass had not been removed before dam closure, which contributed massively to GHG production and emission (Guérin et al., 2006). It is thus highly probable that these reservoirs are not representative for low latitude lakes and reservoirs, as later discussed in detail in Lauerwald et al. (2019).

Similar to their estimates of lake and reservoir CO_2 and CH_4 emissions (see Sections 3 and 4), DelSontro et al. (2018) followed two distinct methodological approaches to obtain their global estimates: a direct upscaling approach based on a global average of observed N_2O emission rates (252–346 Gg $N_2O\,yr^{-1}$), and a statistical approach using lake/reservoir size classes and classes of chlorophyll-a concentrations as predictors

(409–597 Gg N_2O yr^{-1}). Note that the second approach did not lead to a spatially explicit estimate, as only global, statistical distributions of size classes and chlorophyll-a concentrations were used for upscaling. Further, the statistical upscaling equation had a very low predictive power with an R^2 below 0.1.

Deemer et al. (2016) performed a simple upscaling to estimate N_2O emissions from reservoirs only, obtaining a global flux of about 47 Gg N_2O yr^{-1}. Despite the very different approach, Maavara et al. (2019) and Lauerwald et al. (2019) estimated global N_2O emissions from reservoirs that are comparable to those by Deemer et al. (2016) (see Table 4). For the entirety of lakes and reservoirs, Lauerwald et al. (2019) by far the lowest global estimate of 99 ± 64 Gg N_2O yr^{-1}, and which is only about one tenth of what was estimated by Soued et al. (2016). Comparing their spatially explicit estimate to regional estimates based on direct upscaling, Lauerwald et al. (2019) found that their model results are reasonable. Moreover, they estimated that lakes, although contributing more than 90% of the global surface area of standing water bodies, contribute only about half of the emission flux as a result of their much lower average emission rates. This indicates that it is problematic to lump together lakes and reservoirs in global upscaling exercises.

5.2. Persisting Shortcomings and Future Challenges

5.2.1. Process Understanding

In the following we discuss our current process understanding of inland water N_2O emissions in the light of global scale estimates. Figure 2 gives an overview of the main fluxes and processes involved, while Table 2 summarizes the known effects of the major environmental drivers. While a basic understanding of processes involved in aquatic N_2O cycling exists from a certain number of field studies, the quantification of these processes in large-scale estimates is still difficult due to their complexity and the unavailability of sufficient data sets to support their assessment. For this reason, empirical EFs have long been used to estimate riverine N_2O emissions directly from N loads, assuming a constant fraction of N loads to be nitrified and denitrified within the rivers, independent of the size of the river network and its ecoclimatological setting. While newer, model-based studies proved the worth of calculating more precise estimates of nitrification and denitrification fluxes taking into account physical constraints such as water residence time and temperature (Maavara et al., 2019; Marzadri et al., 2021; Yao et al., 2020), the actual production and/or emission of N_2O related to these processes is still based on simple, empirical factors. As N_2O is formed only as a by-product of nitrification and as an intermediate product in the denitrification process, the actual fraction of N_2O produced from these processes is highly variable and not yet possible to reproduce based on mechanistic formulations.

A better assessment of inland water N_2O cycling would require the representation of the vertical profile of oxygen concentrations through the water column and benthic sediments. Of particular importance is the position of the oxycline, that is, the rather narrow zone of steep decrease in oxygen concentrations, separating an oxic upper layer, where nitrification is the dominant process, from an anoxic lower layer, where denitrification dominates. The oxycline itself is a hot-spot of N_2O production because here, anoxic water rich in ammonium mixes with oxygen-rich waters, promoting nitrification, while in turn nitrate produced from nitrification diffuses down and fuels denitrification in the anoxic zone (Beaulieu et al., 2015). Depending on water depth, water column mixing and sediment oxygen consumption, the oxycline lies either in the water column or sediment column. Following the conceptual model by Marzadri et al. (2017, 2021), the position of the oxycline, and thus the relative importance of water column versus sediment processes in N_2O production, changes along the river network. In headwaters, the oxycline is situated in the bed sediments and nitrification of emergent, ammonium-rich groundwater in streambed sediments is the dominant source of N_2O. The importance of nitrification decreases downstream while the oxycline moves up from the sediment into the water column, until finally denitrification in the lower water column is the dominant source of N_2O. Further, it was shown that dissolved N_2O inputs from groundwater and waterlogged soils feed an overproportional contribution of headwaters to riverine N_2O emissions (Billen et al., 2020; Yao et al., 2020). Note that the global assessments of river N_2O emissions by Marzadri et al. (2021) and Maavara et al. (2019) do not account for groundwater N_2O inputs which represent an important part of inland water N_2O emissions.

For lakes and reservoirs, the importance of processes in the benthic zone has been implicitly taken into account by the use of "hydraulic load" to scale denitrification rates (Harrison et al., 2009). Hydraulic load has been defined as the ratio of water inflow to water surface area, which is identical to the ratio of average lake or reservoir

depth over water residence time (Harrison et al., 2009). The process of denitrification is assigned an "apparent settling velocity" which expresses rates of nitrification or denitrification in the benthic zone relative to water column depth. The deeper the average lake or reservoir, the longer it takes until the whole volume is nitrified or denitrified. However, this approach does not take into account the actual shape of the lake/reservoir bed and the proportions of shallow, littoral zones, where the oxycline and thus main source of emitted N_2O lies in the bed sediments (Liikanen et al., 2003; Zhu et al., 2015), versus the deeper zones, where processes in the water column are the dominant source of N_2O (Mengis et al., 1997). While streams and rivers are usually well mixed, deeper lakes and reservoirs may be temporally stratified, with a pronounced oxycline within the water column—and important consequences for N_2O cycling, which have so far not been taken into account in large-scale assessments. During stratification, only the top layer (epilimnion) is exchangeable with the atmosphere and thus well oxygenated. Then, nitrification in the epilimnion is the main source of N_2O emissions (Beaulieu et al., 2015; Mengis et al., 1997). In anoxic parts below the oxycline (hypolimnion), denitrification prevails, which can be a source or sink of N_2O, depending on the availability of nitrate for reduction (Beaulieu et al., 2015; Mengis et al., 1997). As this anoxic water may also be rich in ammonium from the in situ decomposition of organic matter, mixing with more oxygenated, epilimnetic waters during lake turn-over may represent a "hot moment" for nitrification and N_2O emissions (Beaulieu et al., 2015; Roland et al., 2017). However, a quantitative assessment of this hot-moment at large scales is not yet possible due to the lack of observational data. Moreover, while a certain number of studies report measurements of N_2O concentrations in the shallow, easy to reach epilimnion, studies investigating the deeper profile of N_2O concentrations through the hypolimnion are scarce (Beaulieu et al., 2015; Mengis et al., 1997).

Further, also resolving the horizontal zonation would help to better assess the overall N_2O budget of a lake. Within larger lakes, shallow littoral zones have been shown to contribute disproportionately to lake N_2O emissions relative to their areal extent (Zhu et al., 2015). Here, benthic sediments contribute most to N_2O production, while in the deeper, pelagic zone, N_2O is produced in the water column, and more specifically, under stratified conditions with a pronounced oxycline, in the epilimnion (Liikanen et al., 2003; Mengis et al., 1997). Yet, most observations are constrained to pelagic zones, which dominate lakes and reservoirs with regard to surface area, but not necessarily emissions. Further, strong horizontal gradients in N_2O emissions rates may be formed towards the points of riverine inflows of reactive N (Miao et al., 2020). However, few studies conduct systematic sampling which could reveal and account for these internal spatial variations. In contrast to for instance CH_4 or CO_2, drawdown areas of reservoirs do not appear to emit more N_2O than upland soils (Hao et al., 2019). Also, seasonal streambed drying was not found to increase riverine N_2O emissions (Tonina et al., 2021).

In general, observational studies are skewed towards temperate, eutrophic systems in developed countries, which are easily accessible for sampling and which represent potentially important N_2O sources related to water quality issues caused by agricultural non-point sources and sewage water injections. In boreal regions where N loads are usually lower, it was demonstrated that a substantial proportion of aquatic systems is undersaturated with N_2O and thus rather act as sinks for this GHG (Kortelainen et al., 2020; Soued et al., 2016). Further, as for CO_2 and CH_4, observations of smaller water bodies are generally underrepresented. Interestingly, though small, agricultural ponds could be hypothesized to be strong GHG emitters, a study of 101 such systems across Canada (Webb et al., 2019) has shown that about two thirds of these systems are on the contrary N_2O sinks. In conclusion, global inland water N_2O emissions may have been overestimated due to the bias in observed systems outlined above. Moreover, most estimation approaches, particularly the use of EFs, do not permit for representing inland waters as N_2O sinks. Finally, samples from temperate and high latitude systems are skewed towards summer months, while the full seasonal cycle is only rarely covered in observational studies. Kortelainen et al. (2020) have demonstrated in their study on Finnish lakes that there is a strong seasonality in N_2O concentrations and emission rates, with much higher values in winter when low autotrophic production allows for higher nitrate concentrations. A flux estimate based on summer-time observations only would thus have led to an underestimation by a factor of four. Assuming that similar seasonal patterns are to be observed in other temperate to high latitude systems, and that in particular lake turnover as hot moment of N_2O emissions is not well captured in observations, we can hypothesize that the non-representativeness of sampling times might have introduced a negative bias in upscaling exercises. Note finally that the non-representativeness of observations does not only affect estimates based on direct upscaling of average emission rates. With the lack of representative observational data for calibration and validation, also model-based studies will remain of limited validity.

5.2.2. Spatial and Temporal Resolution

For riverine systems, global, spatially explicit estimates of N_2O emissions have been achieved by numerous studies. The spatial resolution ranges from large river basins (Hu et al., 2016), over gridded estimates (Yao et al., 2020) to estimates per stream segment (Marzadri et al., 2021). For lakes, Soued et al. (2016) have resolved N_2O emissions for three broad latitudinal bands and the only published spatially explicit, gridded estimate is that of Lauerwald et al. (2019). Most of these studies represent a climatology of average annual fluxes. Only the process-based model by Yao et al. (2020) allows for spatio-temporally resolved simulation results which cover seasonality, interannual variability and long-term temporal trends. So far, this model includes rivers and reservoirs. For lakes, a global scale, process-based model that permits for temporally varying N_2O emissions is still missing. In line with what was discussed in the preceding subsection, such a model would need to couple lake physics and biogeochemistry.

5.2.3. Data Requirements

To achieve better global estimates of inland water N_2O emissions, more observational data is needed, in particular from high latitude and tropical areas. Also, small lentic water bodies, including natural and farm ponds, and ponds used for aquaculture, are so far undersampled. Finally, the bulk of available observation data is biased by a tendency to study eutrophic systems that promise high emission rates, while oligotrophic systems that may even be sinks are underrepresented (Soued et al., 2016). In general, more systematic observational programs permitting the quantification of seasonality and the impact of seasonal ice cover, lake turn-over and algae blooms to annual emissions are needed to avoid biased upscaling of annual flux estimates. Finally, long-time series are needed to assess the long-term evolution of inland water N_2O emissions and to evaluate process-based models.

To support the application of more advanced upscaling approaches in the estimation of inland water N_2O budgets, including process-based models, better data on environmental drivers and boundary conditions are required. That includes the representation of reactive N species to inland waters. While global estimates of total N and DIN inputs to the river network exist (Mayorga et al., 2010), it would be even better to have information on the more specific inputs of nitrate, ammonium, and dissolved N_2O to set the boundary conditions for processes involved in N_2O production, reduction and emissions. Further, similar to what was pointed out for CH_4 (Section 4.2.3), the model representation of N and N_2O cycling in inland water would profit from data sets on bed morphology of the water body and properties of bed sediments. Marzadri et al. (2021) have used a machine learning approach to estimate all these boundary conditions for the application of their model of stream N_2O production. While this seems a promising strategy, this approach could be steadily improved with new findings from field observations and improved data sets of predictor variables. Also for lakes and reservoirs, only estimates of volume and average lake depth are available (Messager et al., 2016), which could be steadily improved using a similar strategy. Finally, for the better assessment of lake and reservoir N_2O budgets, physical processes such as stratification, mixing and ice cover would need to be represented dynamically. For example, process-based models of lake physical processes have been developed and even implemented into land surface models for global scale application (Subin et al., 2012) and the outputs of such models may be included in future lake and reservoir N_2O models.

6. Conclusions and Outlook

The number of global scale estimates of inland water GHG emissions is constantly increasing, at an accelerated step. For CO_2 and CH_4, we see a tendency for increasing numbers in estimates of global scale fluxes following the inclusion of water bodies which contribute significantly to the overall water surface area, and disproportionally to overall emissions. For water bodies above a certain size (e.g., stream orders, lake size), estimates of average emission rates seem to converge in latest estimates. Major discrepancies persist however with regard to the assumed water surface area and the statistical distribution of water body size classes, in particular for small lakes and impoundments (<10 ha), and ponds. For riverine N_2O emissions on the contrary, we find newer estimates to be lower than older estimates, following a change in methodologies moving away from the application of emission factors toward more process oriented modeling. For lake N_2O emissions, discrepancies in assumed water surface area and distribution of lake size classes still play a role as well, but not as strongly as for CO_2 and CH_4 because small water bodies do not appear to contribute disproportionately to the total emission flux.

While uncertainties in global scale assessment of inland water GHG emissions persist, developments in monitoring and upscaling techniques are envisageable to overcome these uncertainties, as discussed in this review paper and summarized in Table A1. There is ongoing work to improve spatially explicit data sets of inland water surface

areas that will help improve global scale estimates. For streams and rivers, global scale estimates have recently been largely improved combining high resolution remote sensing of water surface areas and statistical prediction for headwater streams which are too narrow to be detected (GRWL—Allen & Pavelsky, 2018). A similar strategy may also be the solution for lakes and reservoirs, combining data from inventories and remote sensing. Inventories are more reliable but less comprehensive as they exclude smallest water bodies and are susceptible to geographical biases due to differences between national data sources. Remote sensing is able to detect smaller water bodies but is prone to contaminations with wrongly attributed water surface areas if unsupervised algorithms are applied and checks for ground truth in sufficient quantity and quality are not possible.

More importantly, improving inland water GHG emissions estimates requires more fieldwork to improve quantity and quality of observational data. In particular, we need more data from systems in remote areas of the high latitudes and the tropics, and systematic measurements with time-series of sufficient length and frequency of observations to better capture seasonal and inter-annual variability in fluxes as well as long-term trends in response to environmental change. In addition, more attention has to be paid to hot-spots and hot-moments of inland water GHG emissions, which likely contribute a substantial fraction of overall emissions.

For upscaling and predictions to achieve better global scale estimates, recent developments of machine learning-based approaches and process-oriented models seem promising. These approaches help to better constrain the spatial-temporal variability in global scale estimates, which allows to better include inland water GHG emissions in regionalized budget efforts such as RECCAP-2, but also in top-down approaches based on atmospheric inversions, further reducing uncertainties in global estimates.

Appendix A

Table A1 summarizes the main take home messages from our review.

Table A1
General Uncertainties and Knowledge Gaps That Persist With Regard to Regional to Global Scale Estimation of Inland Water GHG Emissions, and Recommendations for Monitoring and Upscaling

Uncertainty/knowledge gap	Recommendations for monitoring	Recommendations for upscaling
Source attribution of emitted GHGs difficult: produced in situ or imported from upstream, surrounding soils or groundwater?	Watershed scale monitoring with systematic observations of GHG sources and sinks in interconnected upland, wetland and inland water systems, and of lateral GHG transfers along terrestrial-aquatic continuum.	Process based models that represent sources and sinks of GHGs within the inland waters and their catchment, including the reactive transport along the terrestrial-aquatic continuum.
Smallest water bodies contribute overproportionally to CO_2 and CH_4 emissions, but are not well constrained yet at global scale.	More systematic observations of GHG emissions from small lakes, ponds and streams are needed.	Need for reliable spatial data sets of small inland waters from remote sensing with extensive ground truthing. Categories of climate and land use may be useful for upscaling.
Internal variability needs to be better constrained, especially in large waterbodies with diffuse inputs, and in reservoirs that flood heterogeneous landscapes.	Systematic observations along internal spatial gradients (along depth gradients, distance to shore, position to inflows) are required.	More detailed information on geometry of waterbodies, on inflows of water and sediment, and on reservoir management required to predict internal heterogeneity of GHG fluxes.
Temporal variability (diurnal, event-based, seasonal, interannual) and contributions from hot moments (e.g. spring freshet, flood events, ice-out, lake turn-over, algae blooms, reservoir drawdowns) are poorly constrained at global scale.	Time series of observations needed, which: - are long enough to capture inter-annual variability and the effects of climate extremes such as droughts and heat waves; - are frequent enough to capture hot moments (automatic sensors) -also cover night-time fluxes.	Statistic or process based models that use the main meteorological (temperature, radiation, wind speed, air pressure, precipitation) and hydrodynamic (fluctuations of water flows and water table, thermal stratification vs. mixing over lakes) drivers of the physical and biological processes behind inland water GHG dynamics.
Uneven geographic distribution of observations may lead to biases in upscaling. Higher uncertainties persist for high latitude, high elevation, arid, and tropical systems.	More long-term monitoring networks in remote tropical, arid, high elevation, and high latitude areas are required.	Upscaling techniques are required that bin data per climate zone, or use relevant climatic drivers as predictors or as input for process based models.
Contributions from ebullition versus diffusion, and other paths like emission from turbines not well constrained.	More systematic observations of inland water GHG budgets are needed that cover all important emission paths.	For upscaling, the different emissions paths need to be explicitly represented and their specific drivers taken into account.

Data Availability Statement

The data that support the findings of this study are available at figshare (https://doi.org/10.6084/m9.figshare.22336465.v1).

Acknowledgments

Any use of trade, firm, or product names is for descriptive purposes only and does not imply endorsement by the US Government. Ronny Lauerwald acknowledges funding from French state aid, managed by ANR under the "Investissements d'avenir" programme (ANR-16-CONV-0003) and funding from the European Union's Horizon Europe Research and Innovation programme under Grant Agreement No 101060423. George Allen was funded by a US National Science Foundation CAREER Award (Grant EAR 2145628). Shaoda Liu was funded by the National Key Research and Development Program of China (2021YFC3200401). Matthew Johnson was funded for this work by NASA's Interdisciplinary Research in Earth Science (IDS) Program and the NASA Terrestrial Ecology and Tropospheric Composition Programs. Adam Hastie was funded by Charles University (PRIMUS/23/SCI/013) and NERC (Grant ref. NE/R000751/1). David Bastviken was funded by the European Research Council (ERC; Grant agreement No 725546; METLAKE), the Swedish Research Council (Grant 2016-04829), and FORMAS (Grant 2018-01794). Meredith Holgerson was funded by a US National Science Foundation CAREER Award (Grant DEB 2143449). Pierre Regnier acknowledges funding from the European Union's Horizon 2020 research and innovation program under Grant agreement no. 101003536 (ESM2025—Earth System Models for the Future) and funding from the FRS-FRNS PDR project T.0191.23 CH4-lakes. Alessandra Marzadri acknowledges funding from the Italian Ministry of Education, University and Research (MIUR) in the frame of the Departments of Excellence Initiative 2023–2027 and from the project iNEST - Interconnected Nord-Est Innovation Ecosystem (ECS00000043–CUP E63C22001030007). Lishan Ran was funded by the Research Grants Council of Hong Kong (Grant 17300621). Hanqin Tian acknowledges funding from US National Science Foundation award (Grant 1903722).

References

Aben, R. C. H., Barros, N., van Donk, E., Frenken, T., Hilt, S., Kazanjian, G., et al. (2017). Cross continental increase in methane ebullition under climate change. *Nature Communications*, *8*(1), 1682. https://doi.org/10.1038/s41467-017-01535-y

Abril, G., & Borges, A. V. (2019). Ideas and perspectives: Carbon leaks from flooded land: Do we need to replumb the inland water active pipe? *Biogeosciences*, *16*(3), 769–784. https://doi.org/10.5194/bg-16-769-2019

Abril, G., Bouillon, S., Darchambeau, F., Teodoru, C. R., Marwick, T. R., Tamooh, F., et al. (2015). Technical note: Large overestimation of pCO_2 calculated from pH and alkalinity in acidic, organic-rich freshwaters. *Biogeosciences*, *12*(1), 67–78. https://doi.org/10.5194/bg-12-67-2015

Abril, G., Martinez, J.-M., Artigas, L. F., Moreira-Turcq, P., Benedetti, M. F., Vidal, L., et al. (2014). Amazon River carbon dioxide outgassing fuelled by wetlands. *Nature*, *505*(7483), 395–398. https://doi.org/10.1038/nature12797

Allen, G. H., & Pavelsky, T. (2018). Global extent of rivers and streams. *Science*, *361*(6402), 585–588. https://doi.org/10.1126/science.aat063

Allen, G. H., Pavelsky, T. M., Barefoot, E. A., Lamb, M. P., Butman, D., Tashie, A., & Gleason, C. J. (2018). Similarity of stream width distributions across headwater systems. *Nature Communications*, *9*(1), 610. https://doi.org/10.1038/s41467-018-02991-w

Almeida, R. M., Shi, Q., Gomes-Selman, J. M., Wu, X., Xue, Y., Angarita, H., et al. (2019). Reducing greenhouse gas emissions of Amazon hydropower with strategic dam planning. *Nature Communications*, *10*(1), 4281. https://doi.org/10.1038/s41467-019-12179-5

Anthony, K. W., & MacIntyre, S. (2016). Nocturnal escape route for marsh gas. *Nature*, *535*(7612), 363–365. https://doi.org/10.1038/535363a

Aufdenkampe, A. K., Mayorga, E., Raymond, P. A., Melack, J. M., Doney, S. C., Alin, S. R., et al. (2011). Riverine coupling of biogeochemical cycles between land, oceans, and atmosphere. *Frontiers in Ecology and the Environment*, *9*(1), 53–60. https://doi.org/10.1890/100014

Barbosa, P. M., Melack, J. M., Amaral, J. H. F., Linkhorst, A., & Forsberg, B. R. (2021). Large seasonal and habitat differences in methane ebullition on the Amazon floodplain. *Journal of Geophysical Research: Biogeosciences*, *126*(7), e2020JG005911. https://doi.org/10.1029/2020JG005911

Bastos, A., O'Sullivan, M., Ciais, P., Makowski, D., Sitch, S., Friedlingstein, P., et al. (2020). Sources of uncertainty in regional and global terrestrial CO_2 exchange estimates. *Global Biogeochemical Cycles*, *34*(2). https://doi.org/10.1029/2019GB006393

Bastviken, D., Cole, J., Pace, M., & Tranvik, L. (2004). Methane emissions from lakes: Dependence of lake characteristics, two regional assessments, and a global estimate. *Global Biogeochemical Cycles*, *18*(4), GB4009. https://doi.org/10.1029/2004GB002238

Bastviken, D., Sundgren, I., Natchimuthu, S., Reyier, H., & Gålfalk, M. (2015). Technical note: Cost-efficient approaches to measure carbon dioxide (CO_2) fluxes and concentrations in terrestrial and aquatic environments using mini loggers. *Biogeosciences*, *12*(12), 3849–3859. https://doi.org/10.5194/bg-12-3849-2015

Bastviken, D., Tranvik, L. J., Downing, J. A., Crill, P. M., & Enrich-Prast, A. (2011). Freshwater methane emissions offset the continental carbon sink. *Science*, *331*(6013), 50. https://doi.org/10.1126/science.1196808

Battin, T. J., Lauerwald, R., Bernhardt, E. S., Bertuzzo, E., Gener, L. G., Hall, R. O., et al. (2023). River ecosystem metabolism and carbon biogeochemistry in a changing world. *Nature*, *613*(7944), 449–459. https://doi.org/10.1038/s41586-022-05500-8

Beaulieu, J. J., DelSontro, T., & Downing, J. A. (2019). Eutrophication will increase methane emissions from lakes and impoundments during the 21st century. *Nature Communications*, *10*(1), 1375. https://doi.org/10.1038/s41467-019-09100-5

Beaulieu, J. J., Nietch, C. T., & Young, J. L. (2015). Controls on nitrous oxide production and consumption in reservoirs of the Ohio River Basin. *Journal of Geophysical Research: Biogeosciences*, *120*(10), 1995–2010. https://doi.org/10.1002/2015JG002941

Beaulieu, J. J., Tank Jennifer, L., Hamilton Stephen, K., Wollheim Wilfred, M., Hall Robert, O., Mulholland Patrick, J., et al. (2011). Nitrous oxide emission from denitrification in stream and river networks. *Proceedings of the National Academy of Sciences of the United States of America*, *108*(1), 214–219. https://doi.org/10.1073/pnas.1011464108

Billen, G., Garnier, J., Grossel, A., Thieu, V., Théry, S., & Hénault, C. (2020). Modeling indirect N_2O emissions along the N cascade from cropland soils to rivers. *Biogeochemistry*, *148*(2), 207–221. https://doi.org/10.1007/s10533-020-00654-x

Boereboom, T., Depoorter, M., Coppens, S., & Tison, J. L. (2012). Gas properties of winter lake ice in northern Sweden: Implication for carbon gas release. *Biogeosciences*, *9*(2), 827–838. https://doi.org/10.5194/bg-9-827-2012

Bogard, M. J., & del Giorgio, P. A. (2016). The role of metabolism in modulating CO_2 fluxes in boreal lakes. *Global Biogeochemical Cycles*, *30*(10), 1509–1525. https://doi.org/10.1002/2016GB005463

Borges, A. V., Darchambeau, F., Lambert, T., Morana, C., Allen, G. H., Tambwe, E., et al. (2019). Variations in dissolved greenhouse gases (\chemCO_2, \chemCH_4, \chemN_2O) in the Congo River network overwhelmingly driven by fluvial-wetland connectivity. *Biogeosciences*, *16*(19), 3801–3834. https://doi.org/10.5194/bg-16-3801-2019

Borges, A. V., Darchambeau, F., Teodoru, C. R., Marwick, T. R., Tamooh, F., Geeraert, N., et al. (2015). Globally significant greenhouse-gas emissions from African inland waters. *Nature Geoscience*, *8*(8), 637–642. https://doi.org/10.1038/ngeo2486

Bowring, S. P. K., Lauerwald, R., Guenet, B., Zhu, D., Guimberteau, M., Regnier, P., et al. (2020). ORCHIDEE MICT-LEAK (r5459), a global model for the production, transport, and transformation of dissolved organic carbon from Arctic permafrost regions—Part 2: Model evaluation over the Lena River basin. *Geoscientific Model Development*, *13*(2), 507–520. https://doi.org/10.5194/gmd-13-507-2020

Cael, B., & Seekell, D. (2016). The size-distribution of Earth's lakes. *Scientific Reports*, *6*(1), 29633. https://doi.org/10.1038/srep29633

Calamita, E., Annunziato, S., Gettel Gretchen, M., Franca Mário, J., Scott, W. R., Teodoru Cristian, R., et al. (2021). Unaccounted CO_2 leaks downstream of a large tropical hydroelectric reservoir. *Proceedings of the National Academy of Sciences of the United States of America*, *118*(25), e2026004118. https://doi.org/10.1073/pnas.2026004118

Canadell, J. G., Ciais, P., Gurney, K., Le Quéré, C., Piao, S., Raupach, M. R., & Sabine, C. L. (2011). An international effort to quantify regional carbon fluxes. *EOS*, *92*(10), 81–82. https://doi.org/10.1029/2011eo100001

Canfield, D. E., Glazer, A. N., & Falkowski, P. G. (2010). The evolution and future of Earth's nitrogen cycle. *Science*, *330*(6001), 192–196. https://doi.org/10.1126/science.1186120

Chu, H., Luo, X., Ouyang, Z., Chan, W. S., Dengel, S., Biraud, S. C., et al. (2021). Representativeness of Eddy-Covariance flux footprints for areas surrounding AmeriFlux sites. *Agricultural and Forest Meteorology*, *301–302*, 108350. https://doi.org/10.1016/j.agrformet.2021.108350

Ciais, P., Yao, Y., Gasser, T., Baccini, A., Wang, Y., Lauerwald, R., et al. (2021). Empirical estimates of regional carbon budgets imply reduced global soil heterotrophic respiration. *National Science Review*, *8*(2). https://doi.org/10.1093/nsr/nwaa145

Clough, T. J., Buckthought, L. E., Kelliher, F. M., & Sherlock, R. R. (2007). Diurnal fluctuations of dissolved nitrous oxide (N_2O) concentrations and estimates of N_2O emissions from a spring-fed river: Implications for IPCC methodology. *Global Change Biology*, *13*(5), 1016–1027. https://doi.org/10.1111/j.1365-2486.2007.01337.x

Colas, F., Chanudet, V., Daufresne, M., Buchet, L., Vigouroux, R., Bonnet, A., et al. (2020). Spatial and temporal variability of diffusive CO_2 and CH_4 fluxes from the Amazonian reservoir Petit-Saut (French Guiana) reveals the importance of allochthonous inputs for long-term C emissions. *Global Biogeochemical Cycles*, *34*(12), e2020GB006602. https://doi.org/10.1029/2020GB006602

Cole, J. J., & Caraco, N. F. (1998). Atmospheric exchange of carbon dioxide in a low-wind oligotrophic lake measured by the addition of SF6. *Limnology & Oceanography*, *43*(4), 647–656. https://doi.org/10.4319/lo.1998.43.4.0647

Cole, J. J., Caraco, N. F., & Caraco, N. F. (2001). Carbon in catchments: Connecting terrestrial carbon losses with aquatic metabolism. *Marine and Freshwater Research*, *52*(1), 101–110. https://doi.org/10.1071/MF00084

Cole, J. J., Prairie, Y. T., Caraco, N. F., McDowell, W. H., Tranvik, L. J., Striegl, R. G., et al. (2007). Plumbing the global carbon cycle: Integrating inland waters into the terrestrial carbon budget. *Ecosystems*, *10*(1), 172–185. https://doi.org/10.1007/s10021-006-9013-8

Couto, T. B., & Olden, J. D. (2018). Global proliferation of small hydropower plants—Science and policy. *Frontiers in Ecology and the Environment*, *16*(2), 91–100. https://doi.org/10.1002/fee.1746

Crawford, J. T., Lottig, N. R., Stanley, E. H., Walker, J. F., Hanson, P. C., Finlay, J. C., & Striegl, R. G. (2014). CO_2 and CH_4 emissions from streams in a lake-rich landscape: Patterns, controls, and regional significance. *Global Biogeochemical Cycles*, *28*(3), 197–210. https://doi.org/10.1002/2013GB004661

Crawford, J. T., Stanley, E. H., Spawn, S. A., Finlay, J. C., Loken, L. C., & Striegl, R. G. (2014). Ebullitive methane emissions from oxygenated wetland streams. *Global Change Biology*, *20*(11), 3408–3422. https://doi.org/10.1111/gcb.12614

D'Ambrosio, S. L., & Harrison, J. A. (2021). Methanogenesis exceeds CH_4 consumption in eutrophic lake sediments. *Limnology and Oceanography Letters*, *6*(4), 173–181. https://doi.org/10.1002/lol2.10192

Davidson, T. A., Audet, J., Jeppesen, E., Landkildehus, F., Lauridsen, T. L., Søndergaard, M., & Syväranta, J. (2018). Synergy between nutrients and warming enhances methane ebullition from experimental lakes. *Nature Climate Change*, *8*(2), 156–160. https://doi.org/10.1038/s41558-017-0063-z

Davidson, T. A., Audet, J., Svenning, J.-C., Lauridsen, T. L., Søndergaard, M., Landkildehus, F., et al. (2015). Eutrophication effects on greenhouse gas fluxes from shallow-lake mesocosms override those of climate warming. *Global Change Biology*, *21*(12), 4449–4463. https://doi.org/10.1111/gcb.13062

Deemer, B., & Holgerson, M. A. (2021). Drivers of methane flux differ between lakes and reservoirs, complicating global upscaling efforts. *Journal of Geophysical Research-Biogeosciences*, *126*(4), e2019JG005600. https://doi.org/10.1029/2019JG005600

Deemer, B. R., Harrison, J. A., Li, S., Beaulieu, J. J., DelSontro, T., Barros, N., et al. (2016). Greenhouse gas emissions from reservoir water surfaces: A new global synthesis. *BioScience*, *66*(11), 949–964. https://doi.org/10.1093/biosci/biw117

De Klein, C., Novoa, R. S., Ogle, S., Smith, K. A., Rochette, P., Wirth, T. C., et al. (2006). N_2O emissions from managed soils, and CO_2 emissions from lime and urea application. In *IPCC guidelines for national greenhouse gas inventories, prepared by the national greenhouse gas inventories programme* (Vol. 4, pp. 11.01–11.54).

DelSontro, T., Beaulieu, J. J., & Downing, J. A. (2018). Greenhouse gas emissions from lakes and impoundments: Upscaling in the face of global change. *Limnology and Oceanography Letters*, *3*(3), 64–75. https://doi.org/10.1002/lol2.10073

DelSontro, T., Kunz, M. J., Kempter, T., Wüest, A., Wehrli, B., & Senn, D. B. (2011). Spatial heterogeneity of methane ebullition in a large tropical reservoir. *Environmental Science & Technology*, *45*(23), 9866–9873. https://doi.org/10.1021/es2005545

Delwiche, K., & Hemond, H. F. (2017). An enhanced bubble size sensor for long-term ebullition studies. *Limnology and Oceanography: Methods*, *15*(10), 821–835. https://doi.org/10.1002/lom3.10201

Delwiche, K. B., Harrison, J. A., Maasakkers, J. D., Sulprizio, M. P., Worden, J., Jacob, D. J., & Sunderland, E. M. (2022). Estimating drivers and pathways for hydroelectric reservoir methane emissions using a new mechanistic model. *Journal of Geophysical Research: Biogeosciences*, *127*(8), e2022JG006908. https://doi.org/10.1029/2022JG006908

Denfeld, B. A., Baulch, H. M., del Giorgio, P. A., Hampton, S. E., & Karlsson, J. (2018). A synthesis of carbon dioxide and methane dynamics during the ice-covered period of northern lakes. *Limnology and Oceanography Letters*, *3*(3), 117–131. https://doi.org/10.1002/lol2.10079

Downing, J. A., Cole, J. J., Duarte, C. M., Middelburg, J. J., Melack, J. M., Prairie, Y. T., et al. (2012). Global abundance and size distribution of streams and rivers. *Inland Waters*, *2*(4), 229–236. https://doi.org/10.5268/IW-2.4.502

Downing, J. A., Prairie, Y. T., Cole, J. J., Duarte, C. M., Tranvik, L. J., Striegl, R. G., et al. (2006). The global abundance and size distribution of lakes, ponds, and impoundments. *Limnology & Oceanography*, *51*(5), 2388–2397. https://doi.org/10.4319/lo.2006.51.5.2388

Downing, J. A., & Striegl, R. G. (2018). Size, age, renewal, and discharge of groundwater carbon. *Inland Waters*, *8*(1), 122–127. https://doi.org/10.1080/20442041.2017.1412918

Duc, N. T., Crill, P., & Bastviken, D. (2010). Implications of temperature and sediment characteristics on methane formation and oxidation in lake sediments. *Biogeochemistry*, *100*(1–3), 185–196. https://doi.org/10.1007/s10533-010-9415-8

Engram, M., Walter Anthony, K. M., Sachs, T., Kohnert, K., Serafimovich, A., Grosse, G., & Meyer, F. J. (2020). Remote sensing northern lake methane ebullition. *Nature Climate Change*, *10*(6), 511–517. https://doi.org/10.1038/s41558-020-0762-8

Eugster, W., DelSontro, T., & Sobek, S. (2011). Eddy covariance flux measurements confirm extreme CH_4 emissions from a Swiss hydropower reservoir and resolve their short-term variability. *Biogeosciences*, *8*(9), 2815–2831. https://doi.org/10.5194/bg-8-2815-2011

Finlay, J. C. (2003). Controls of streamwater dissolved inorganic carbon dynamics in a forested watershed. *Biogeochemistry*, *62*(3), 231–252. https://doi.org/10.1023/A:1021183023963

Godwin, C. M., McNamara, P. J., & Markfort, C. D. (2013). Evening methane emission pulses from a boreal wetland correspond to convective mixing in hollows. *Journal of Geophysical Research: Biogeosciences*, *118*(3), 994–1005. https://doi.org/10.1002/jgrg.20082

Golub, M., Desai, A. R., McKinley, G. A., Remucal, C. K., & Stanley, E. H. (2017). Large uncertainty in estimating pCO_2 from carbonate equilibria in lakes. *Journal of Geophysical Research: Biogeosciences*, *122*(11), 2909–2924. https://doi.org/10.1002/2017JG003794

Gómez-Gener, L., Rocher-Ros, G., Battin, T., Cohen, M. J., Dalmagro, H. J., Dinsmore, K. J., et al. (2021). Global carbon dioxide efflux from rivers enhanced by high nocturnal emissions. *Nature Geoscience*, *14*(5), 289–294. https://doi.org/10.1038/s41561-021-00722-3

Gommet, C., Lauerwald, R., Ciais, P., Guenet, B., Zhang, H., & Regnier, P. (2022). Spatiotemporal patterns and drivers of terrestrial dissolved organic carbon (DOC) leaching into the European river network. *Earth System Dynamics*, *13*(1), 393–418. https://doi.org/10.5194/esd-13-393-2022

Grasset, C., Sobek, S., Scharnweber, K., Moras, S., Villwock, H., Andersson, S., et al. (2020). The CO_2-equivalent balance of freshwater ecosystems is non-linearly related to productivity. *Global Change Biology*, *26*(10), 5705–5715. https://doi.org/10.1111/gcb.15284

Grilli, R., Darchambeau, F., Chappellaz, J., Mugisha, A., Triest, J., & Umutoni, A. (2020). Continuous in situ measurement of dissolved methane in Lake Kivu using a membrane inlet laser spectrometer. *Geoscientific Instrumentation, Methods and Data Systems*, *9*(1), 141–151. https://doi.org/10.5194/gi-9-141-2020

Grinham, A., Albert, S., Deering, N., Dunbabin, M., Bastviken, D., Sherman, B., et al. (2018). The importance of small artificial water bodies as sources of methane emissions in Queensland, Australia. *Hydrology and Earth System Sciences*, *22*(10), 5281–5298. https://doi.org/10.5194/hess-22-5281-2018

Grinham, A., Dunbabin, M., Gale, D., & Udy, J. (2011). Quantification of ebullitive and diffusive methane release to atmosphere from a water storage. *Atmospheric Environment*, *45*(39), 7166–7173. https://doi.org/10.1016/j.atmosenv.2011.09.011

Guérin, F., Abril, G., Richard, S., Burban, B., Reynouard, C., Seyler, P., & Delmas, R. (2006). Methane and carbon dioxide emissions from tropical reservoirs: Significance of downstream rivers. *Geophysical Research Letters*, *33*(21), L21407. https://doi.org/10.1029/2006GL027929

Hao, Q., Chen, S., Ni, X., Li, X., He, X., & Jiang, C. (2019). Methane and nitrous oxide emissions from the drawdown areas of the Three Gorges Reservoir. *Science of the Total Environment*, *660*, 567–576. https://doi.org/10.1016/j.scitotenv.2019.01.050

Harrison, J. A., Deemer, B. R., Birchfield, M. K., & O'Malley, M. T. (2017). Reservoir water-level drawdowns accelerate and amplify methane emission. *Environmental Science & Technology*, *51*(3), 1267–1277. https://doi.org/10.1021/acs.est.6b03185

Harrison, J. A., Maranger, R. J., Alexander, R. B., Giblin, A. E., Jacinthe, P.-A., Mayorga, E., et al. (2009). The regional and global significance of nitrogen removal in lakes and reservoirs. *Biogeochemistry*, *93*(1–2), 143–157. https://doi.org/10.1007/s10533-008-9272-x

Harrison, J. A., Prairie, Y. T., Mercier-Blais, S., & Soued, C. (2021). Year-2020 global distribution and pathways of reservoir methane and carbon dioxide emissions according to the greenhouse gas from reservoirs (G-res) model. *Global Biogeochemical Cycles*, *35*(6), e2020GB006888. https://doi.org/10.1029/2020GB006888

Hartmann, J., Lauerwald, R., & Moosdorf, N. (2014). A brief overview of the GLObal RIver chemistry database, GLORICH. *Geochemistry of the Earth's Surface GES-10 Paris France*, *10*, 23–27. https://doi.org/10.1016/j.proeps.2014.08.005

Hastie, A., Lauerwald, R., Ciais, P., Papa, F., & Regnier, P. (2021). Historical and future contributions of inland waters to the Congo Basin carbon balance. *Earth System Dynamics*, *12*(1), 37–62. https://doi.org/10.5194/esd-12-37-2021

Hastie, A., Lauerwald, R., Weyhenmeyer, G., Sobek, S., Verpoorter, C., & Regnier, P. (2018). CO_2 evasion from boreal lakes: Revised estimate, drivers of spatial variability, and future projections. *Global Change Biology*, *24*(2), 711–728. https://doi.org/10.1111/gcb.13902

Holgerson, M. A., & Raymond, P. A. (2016). Large contribution to inland water CO_2 and CH_4 emissions from very small ponds. *Nature Geoscience*, *9*(3), 222–226. https://doi.org/10.1038/ngeo2654

Horgby, Å., Segatto, P. L., Bertuzzo, E., Lauerwald, R., Lehner, B., Ulseth, A. J., et al. (2019). Unexpected large evasion fluxes of carbon dioxide from turbulent streams draining the world's mountains. *Nature Communications*, *10*(1), 4888. https://doi.org/10.1038/s41467-019-12905-z

Hotchkiss, E. R., Hall, R. O., Jr., Sponseller, R. A., Butman, D., Klaminder, J., Laudon, H., et al. (2015). Sources of and processes controlling CO_2 emissions change with the size of streams and rivers. *Nature Geoscience*, *8*(9), 696–699. https://doi.org/10.1038/ngeo2507

Hu, M., Chen, D., & Dahlgren, R. A. (2016). Modeling nitrous oxide emission from rivers: A global assessment. *Global Change Biology*, *22*(11), 3566–3582. https://doi.org/10.1111/gcb.13351

Hu, M., Liu, Y., Zhang, Y., Dahlgren, R. A., & Chen, D. (2019). Coupling stable isotopes and water chemistry to assess the role of hydrological and biogeochemical processes on riverine nitrogen sources. *Water Research*, *150*, 418–430. https://doi.org/10.1016/j.watres.2018.11.082

Humborg, C., Mörth, C.-M., Sundbom, M., Borg, H., Blenckner, T., Giesler, R., & Ittekkot, V. (2010). CO_2 supersaturation along the aquatic conduit in Swedish watersheds as constrained by terrestrial respiration, aquatic respiration and weathering. *Global Change Biology*, *16*(7), 1966–1978. https://doi.org/10.1111/j.1365-2486.2009.02092.x

Hunt, C. W., Salisbury, J. E., & Vandemark, D. (2011). Contribution of non-carbonate anions to total alkalinity and overestimation of pCO_2 in New England and New Brunswick rivers. *Biogeosciences*, *8*(10), 3069–3076. https://doi.org/10.5194/bg-8-3069-2011

IPCC. (2013). In T. F. Stocker, D. Qin, G.-K. Plattner, M. Tignor, S. K. Allen, J. Boschung, et al. (Eds.), *Climate change 2013: The physical science basis. Contribution of working group I to the fifth assessment report of the intergovernmental panel on climate change* (p. 1535). Cambridge University Press.

IPCC. (2021). In V. Masson-Delmotte, P. Zhai, A. Pirani, S. L. Connors, C. Péan, S. Berger, et al. (Eds.), *Climate change 2021. The physical science basis. Contribution of working group I to the sixth assessment report of the intergovernmental panel on climate change* (p. 2391). Cambridge University Press.

Jansen, J., Woolway, R. I., Kraemer, B. M., Albergel, C., Bastviken, D., Weyhenmeyer, G. A., et al. (2022). Global increase in methane production under future warming of lake bottom waters. *Global Change Biology*, *28*(18), 5427–5440. https://doi.org/10.1111/gcb.16298

Johnson, M. S., Lehmann, J., Riha, S. J., Krusche, A. V., Richey, J. E., Ometto, J. P. H. B., & Couto, E. G. (2008). CO_2 efflux from Amazonian headwater streams represents a significant fate for deep soil respiration. *Geophysical Research Letters*, *35*(17), L17401. https://doi.org/10.1029/2008GL034619

Johnson, M. S., Matthews, E., Bastviken, D., Deemer, B., Du, J., & Genovese, V. (2021). Spatiotemporal methane emission from global reservoirs. *Journal of Geophysical Research: Biogeosciences*, *126*(8), e2021JG006305. https://doi.org/10.1029/2021JG006305

Johnson, M. S., Matthews, E., Du, J., Genovese, V., & Bastviken, D. (2022). Methane emission from global lakes: New spatiotemporal data and observation-driven modeling of methane dynamics indicates lower emissions. *Journal of Geophysical Research: Biogeosciences*, *127*(7), e2022JG006793. https://doi.org/10.1029/2022JG006793

Jones, J. B., Jr., Stanley, E. H., & Mulholland, P. J. (2003). Long-term decline in carbon dioxide supersaturation in rivers across the contiguous United States. *Geophysical Research Letters*, *30*(10), 1495. https://doi.org/10.1029/2003GL017056

Joyce, J., & Jewell, P. W. (2003). Physical controls on methane ebullition from reservoirs and lakes. *Environmental and Engineering Geoscience*, *9*(2), 167–178. https://doi.org/10.2113/9.2.167

Jurado, A., Borges, A. V., & Brouyère, S. (2017). Dynamics and emissions of N_2O in groundwater: A review. *Science of the Total Environment*, *584*(585), 207–218. https://doi.org/10.1016/j.scitotenv.2017.01.127

Karlsson, J., Serikova, S., Vorobyev, S. N., Rocher-Ros, G., Denfeld, B., & Pokrovsky, O. S. (2021). Carbon emission from western Siberian inland waters. *Nature Communications*, *12*(1), 825. https://doi.org/10.1038/s41467-021-21054-1

Keller, P. S., Catalán, N., von Schiller, D., Grossart, H.-P., Koschorreck, M., Obrador, B., et al. (2020). Global CO_2 emissions from dry inland waters share common drivers across ecosystems. *Nature Communications*, *11*(1), 2126. https://doi.org/10.1038/s41467-020-15929-y

Keller, P. S., Marcé, R., Obrador, B., & Koschorreck, M. (2021). Global carbon budget of reservoirs is overturned by the quantification of drawdown areas. *Nature Geoscience*, *14*(6), 402–408. https://doi.org/10.1038/s41561-021-00734-z

Kortelainen, P., Larmola, T., Rantakari, M., Juutinen, S., Alm, J., & Martikainen, P. J. (2020). Lakes as nitrous oxide sources in the boreal landscape. *Global Change Biology*, *26*(3), 1432–1445. https://doi.org/10.1111/gcb.14928

Kroeze, C., Dumont, E., & Seitzinger, S. (2010). Future trends in emissions of N_2O from rivers and estuaries. *Journal of Integrative Environmental Sciences*, *7*(1), 71–78. https://doi.org/10.1080/1943815X.2010.496789

Kroeze, C., Dumont, E., & Seitzinger, S. P. (2005). New estimates of global emissions of N_2O from rivers and estuaries. *Environmental Sciences*, *2*(2–3), 159–165. https://doi.org/10.1080/15693430500384671

Kuhn, M. A., Varner, R. K., Bastviken, D., Crill, P., MacIntyre, S., Turetsky, M., et al. (2021). BAWLD-CH4: A comprehensive dataset of methane fluxes from boreal and arctic ecosystems. *Earth System Science Data*, *13*(11), 5151–5189. https://doi.org/10.5194/essd-13-5151-2021

Lapierre, J.-F., Guillemette, F., Berggren, M., & del Giorgio, P. A. (2013). Increases in terrestrially derived carbon stimulate organic carbon processing and CO_2 emissions in boreal aquatic ecosystems. *Nature Communications*, *4*(1), 2972. https://doi.org/10.1038/ncomms3972

Lauerwald, R., Allen, G. H., Deemer, B. R., Liu, S., Maavara, T., Raymond, P., et al. (2023). Inland water greenhouse gas budgets for RECCAP2: 2. Regionalization and homogenization of estimates.

Lauerwald, R., Laruelle, G. G., Hartmann, J., Ciais, P., & Regnier, P. A. G. (2015). Spatial patterns in CO_2 evasion from the global river network. *Global Biogeochemical Cycles*, *29*(5), 534–554. https://doi.org/10.1002/2014GB004941

Lauerwald, R., Regnier, P., Camino-Serrano, M., Guenet, B., Guimberteau, M., Ducharne, A., et al. (2017). ORCHILEAK (revision 3875): A new model branch to simulate carbon transfers along the terrestrial-aquatic continuum of the Amazon basin. *Geoscientific Model Development*, *10*(10), 3821–3859. https://doi.org/10.5194/gmd-10-3821-2017

Lauerwald, R., Regnier, P., Figueiredo, V., Enrich-Prast, A., Bastviken, D., Lehner, B., et al. (2019). Natural lakes are a minor global source of N_2O to the atmosphere. *Global Biogeochemical Cycles*, *33*(12), 1564–1581. https://doi.org/10.1029/2019GB006261

Lauerwald, R., Regnier, P., Guenet, B., Friedlingstein, P., & Ciais, P. (2020). How simulations of the land carbon sink are biased by ignoring fluvial carbon transfers: A case study for the Amazon basin. *One Earth*, *3*(2), 226–236. https://doi.org/10.1016/j.oneear.2020.07.009

Lehner, B., & Döll, P. (2004). Development and validation of a global database of lakes, reservoirs and wetlands. *Journal of Hydrology*, *296*(1), 1–22. https://doi.org/10.1016/j.jhydrol.2004.03.028

Lehner, B., & Grill, G. (2013). Global river hydrography and network routing: Baseline data and new approaches to study the world's large river systems. *Hydrological Processes*, *27*(15), 2171–2186. https://doi.org/10.1002/hyp.9740

Lehner, B., Liermann, C. R., Revenga, C., Vörösmarty, C., Fekete, B., Crouzet, P., et al. (2011). High-resolution mapping of the world's reservoirs and dams for sustainable river-flow management. *Frontiers in Ecology and the Environment*, *9*(9), 494–502. https://doi.org/10.1890/100125

Lehner, B., Verdin, K., & Jarvis, A. (2008). New global hydrography derived from spaceborne elevation data. *Eos, Transactions American Geophysical Union*, *89*(10), 93–94. https://doi.org/10.1029/2008EO100001

Liikanen, A., Huttunen, J. T., Murtoniemi, T., Tanskanen, H., Väisänen, T., Silvola, J., et al. (2003). Spatial and seasonal variation in greenhouse gas and nutrient dynamics and their interactions in the sediments of a boreal eutrophic lake. *Biogeochemistry*, *65*(1), 83–103. https://doi.org/10.1023/A:1026070209387

Lin, P., Pan, M., Wood, E. F., Yamazaki, D., & Allen, G. H. (2021). A new vector-based global river network dataset accounting for variable drainage density. *Scientific Data*, *8*(1), 28. https://doi.org/10.1038/s41597-021-00819-9

Linkhorst, A., Hiller, C., DelSontro, T., Azevedo, G. M., Barros, N., Mendonça, R., & Sobek, S. (2020). Comparing methane ebullition variability across space and time in a Brazilian reservoir. *Limnology & Oceanography*, *65*(7), 1623–1634. https://doi.org/10.1002/lno.11410

Liu, S., Butman, D. E., & Raymond, P. A. (2020). Evaluating CO_2 calculation error from organic alkalinity and pH measurement error in low ionic strength freshwaters. *Limnology and Oceanography: Methods*, *18*(10), 606–622. https://doi.org/10.1002/lom3.10388

Liu, S., Kuhn, C., Amatulli, G., Aho, K., Butman, D. E., Allen, G. H., et al. (2022). The importance of hydrology in routing terrestrial carbon to the atmosphere via global streams and rivers. *Proceedings of the National Academy of Sciences of the United States of America*, *119*(11), e2106322119. https://doi.org/10.1073/pnas.2106322119

Lorke, A., Bodmer, P., Noss, C., Alshboul, Z., Koschorreck, M., Somlai-Haase, C., et al. (2015). Technical note: Drifting versus anchored flux chambers for measuring greenhouse gas emissions from running waters. *Biogeosciences*, *12*(23), 7013–7024. https://doi.org/10.5194/bg-12-7013-2015

Maavara, T., Lauerwald, R., Laruelle, G. G., Akbarzadeh, Z., Bouskill, N. J., Van Cappellen, P., & Regnier, P. (2019). Nitrous oxide emissions from inland waters: Are IPCC estimates too high? *Global Change Biology*, *25*(2), 473–488. https://doi.org/10.1111/gcb.14504

MacIntyre, S., Bastviken, D., Arneborg, L., Crowe, A. T., Karlsson, J., Andersson, A., et al. (2021). Turbulence in a small boreal lake: Consequences for air–water gas exchange. *Limnology & Oceanography*, *66*(3), 827–854. https://doi.org/10.1002/lno.11645

Maeck, A., DelSontro, T., McGinnis, D. F., Fischer, H., Flury, S., Schmidt, M., et al. (2013). Sediment trapping by dams creates methane emission hot spots. *Environmental Science & Technology*, *47*(15), 8130–8137. https://doi.org/10.1021/es4003907

Marcé, R., Obrador, B., Gómez-Gener, L., Catalán, N., Koschorreck, M., Arce, M. I., et al. (2019). Emissions from dry inland waters are a blind spot in the global carbon cycle. *Earth-Science Reviews*, *188*, 240–248. https://doi.org/10.1016/j.earscirev.2018.11.012

Marx, A., Dusek, J., Jankovec, J., Sanda, M., Vogel, T., van Geldern, R., et al. (2017). A review of CO_2 and associated carbon dynamics in headwater streams: A global perspective. *Reviews of Geophysics*, *55*(2), 560–585. https://doi.org/10.1002/2016RG000547

Marzadri, A., Amatulli, G., Tonina, D., Bellin, A., Shen, L. Q., Allen, G. H., & Raymond, P. A. (2021). Global riverine nitrous oxide emissions: The role of small streams and large rivers. *Science of the Total Environment*, *776*, 145148. https://doi.org/10.1016/j.scitotenv.2021.145148

Marzadri, A., Dee, M. M., Tonina, D., Bellin, A., & Tank, J. L. (2017). Role of surface and subsurface processes in scaling N_2O emissions along riverine networks. *Proceedings of the National Academy of Sciences of the United States of America*, *114*(17), 4330–4335. https://doi.org/10.1073/pnas.1617454114

Matthews, E., Johnson, M. S., Genovese, V., Du, J., & Bastviken, D. (2020). Methane emission from high latitude lakes: Methane-centric lake classification and satellite-driven annual cycle of emissions. *Scientific Reports*, *10*(1), 12465. https://doi.org/10.1038/s41598-020-68246-1

Mattson, M. D., & Likens, G. E. (1990). Air pressure and methane fluxes. *Nature*, *347*(6295), 718–719. https://doi.org/10.1038/347718b0

Mayorga, E., Seitzinger, S. P., Harrison, J. A., Dumont, E., Beusen, A. H. W., Bouwman, A. F., et al. (2010). Global nutrient export from WaterSheds 2 (NEWS 2): Model development and implementation. *Environmental Modelling & Software*, *25*(7), 837–853. https://doi.org/10.1016/j.envsoft.2010.01.007

Mayr, M. J., Zimmermann, M., Dey, J., Brand, A., Wehrli, B., & Bürgmann, H. (2020). Growth and rapid succession of methanotrophs effectively limit methane release during lake overturn. *Communications Biology*, *3*(1), 108. https://doi.org/10.1038/s42003-020-0838-z

Mengis, M., Gächter, R., & Wehrli, B. (1997). Sources and sinks of nitrous oxide (N_2O) in deep lakes. *Biogeochemistry*, *38*(3), 281–301. https://doi.org/10.1023/A:1005814020322

Messager, M. L., Lehner, B., Cockburn, C., Lamouroux, N., Pella, H., Snelder, T., et al. (2021). Global prevalence of non-perennial rivers and streams. *Nature*, *594*(7863), 391–397. https://doi.org/10.1038/s41586-021-03565-5

Messager, M. L., Lehner, B., Grill, G., Nedeva, I., & Schmitt, O. (2016). Estimating the volume and age of water stored in global lakes using a geo-statistical approach. *Nature Communications*, *7*(1), 13603. https://doi.org/10.1038/ncomms13603

Miao, Y., Huang, J., Duan, H., Meng, H., Wang, Z., Qi, T., & Wu, Q. L. (2020). Spatial and seasonal variability of nitrous oxide in a large freshwater lake in the lower reaches of the Yangtze River, China. *Science of the Total Environment*, *721*, 137716. https://doi.org/10.1016/j.scitotenv.2020.137716

Mosier, A., Kroeze, C., Nevison, C., Oenema, O., Seitzinger, S., & van Cleemput, O. (1998). Closing the global N_2O budget: Nitrous oxide emissions through the agricultural nitrogen cycle. *Nutrient Cycling in Agroecosystems*, *52*(2), 225–248. https://doi.org/10.1023/A:1009740530221

Müller, D., Warneke, T., Rixen, T., Müller, M., Jamahari, S., Denis, N., et al. (2015). Lateral carbon fluxes and CO_2 outgassing from a tropical peat-draining river. *Biogeosciences*, *12*(20), 5967–5979. https://doi.org/10.5194/bg-12-5967-2015

Mulligan, M., van Soesbergen, A., & Sáenz, L. (2020). GOODD, a global dataset of more than 38,000 georeferenced dams. *Scientific Data*, *7*(1), 31. https://doi.org/10.1038/s41597-020-0362-5

Natchimuthu, S., Sundgren, I., Gålfalk, M., Klemedtsson, L., & Bastviken, D. (2017). Spatiotemporal variability of lake pCO_2 and CO_2 fluxes in a hemiboreal catchment. *Journal of Geophysical Research: Biogeosciences*, *122*(1), 30–49. https://doi.org/10.1002/2016JG003449

Natchimuthu, S., Sundgren, I., Gålfalk, M., Klemedtsson, L., Crill, P., Danielsson, Å., & Bastviken, D. (2016). Spatio-temporal variability of lake CH_4 fluxes and its influence on annual whole lake emission estimates. *Limnology & Oceanography*, *61*(S1), S13–S26. https://doi.org/10.1002/lno.10222

Natchimuthu, S., Wallin, M. B., Klemedtsson, L., & Bastviken, D. (2017). Spatio-temporal patterns of stream methane and carbon dioxide emissions in a hemiboreal catchment in southwest Sweden. *Scientific Reports*, *7*(1), 39729. https://doi.org/10.1038/srep39729

O'Connor, D. J., & Dobbins, W. E. (1958). Mechanism of reaeration in natural streams. *Transactions of the American Society of Civil Engineers*, *123*(1), 641–666. https://doi.org/10.1061/taceat.0007609

Ostrovsky, I., McGinnis, D. F., Lapidus, L., & Eckert, W. (2008). Quantifying gas ebullition with echosounder: The role of methane transport by bubbles in a medium-sized lake. *Limnology and Oceanography: Methods*, *6*(2), 105–118. https://doi.org/10.4319/lom.2008.6.105

Outram, F. N., & Hiscock, K. M. (2012). Indirect nitrous oxide emissions from surface water bodies in a lowland arable catchment: A significant contribution to agricultural greenhouse gas budgets? *Environmental Science & Technology*, *46*(15), 8156–8163. https://doi.org/10.1021/es3012244

Paranaíba, J. R., Aben, R., Barros, N., Quadra, G., Linkhorst, A., Amado, A. M., et al. (2022). Cross-continental importance of CH_4 emissions from dry inland-waters. *Science of the Total Environment*, *814*, 151925. https://doi.org/10.1016/j.scitotenv.2021.151925

Peixoto, R., Machado-Silva, F., Marotta, H., Enrich-Prast, A., & Bastviken, D. (2015). Spatial versus day-to-day within-lake variability in tropical floodplain lake CH_4 emissions—Developing optimized approaches to representative flux measurements. *PLoS One*, *10*(4), e0123319. https://doi.org/10.1371/journal.pone.0123319

Pekel, J.-F., Cottam, A., Gorelick, N., & Belward, A. S. (2016). High-resolution mapping of global surface water and its long-term changes. *Nature*, *540*(7633), 418–422. https://doi.org/10.1038/nature20584

Pi, X., Luo, Q., Feng, L., Xu, Y., Tang, J., Liang, X., et al. (2022). Mapping global lake dynamics reveals the emerging roles of small lakes. *Nature Communications*, *13*(1), 5777. https://doi.org/10.1038/s41467-022-33239-3

Pickens, A. H., Hansen, M. C., Hancher, M., Stehman, S. V., Tyukavina, A., Potapov, P., et al. (2020). Mapping and sampling to characterize global inland water dynamics from 1999 to 2018 with full Landsat time-series. *Remote Sensing of Environment*, *243*, 111792. https://doi.org/10.1016/j.rse.2020.111792

Podgrajsek, E., Sahlée, E., Bastviken, D., Holst, J., Lindroth, A., Tranvik, L., & Rutgersson, A. (2014). Comparison of floating chamber and eddy covariance measurements of lake greenhouse gas fluxes. *Biogeosciences*, *11*(15), 4225–4233. https://doi.org/10.5194/bg-11-4225-2014

Poindexter, C. M., Baldocchi, D. D., Matthes, J. H., Knox, S. H., & Variano, E. A. (2016). The contribution of an overlooked transport process to a wetland's methane emissions. *Geophysical Research Letters*, *43*(12), 6276–6284. https://doi.org/10.1002/2016GL068782

Prairie, Y. T., Mercier-Blais, S., Harrison, J. A., Soued, C., del Giorgio, P., Harby, A., et al. (2021). A new modelling framework to assess biogenic GHG emissions from reservoirs: The G-res tool. *Environmental Modelling & Software*, *143*, 105117. https://doi.org/10.1016/j.envsoft.2021.105117

Ran, L., Butman, D. E., Battin, T. J., Yang, X., Tian, M., Duvert, C., et al. (2021). Substantial decrease in CO_2 emissions from Chinese inland waters due to global change. *Nature Communications*, *12*(1), 1730. https://doi.org/10.1038/s41467-021-21926-6

Rasilo, T., Hutchins, R. H. S., Ruiz-González, C., & del Giorgio, P. A. (2017). Transport and transformation of soil-derived CO_2, CH_4 and DOC sustain CO_2 supersaturation in small boreal streams. *Science of the Total Environment*, *579*, 902–912. https://doi.org/10.1016/j.scitotenv.2016.10.187

Raymond, P. A., Hartmann, J., Lauerwald, R., Sobek, S., McDonald, C., Hoover, M., et al. (2013). Global carbon dioxide emissions from inland waters. *Nature*, *503*(7476), 355–359. https://doi.org/10.1038/nature12760

Raymond, P. A., Zappa, C. J., Butman, D. E., Bott, T. L., Potter, J. D., Mulholland, P. J., et al. (2012). Scaling the gas transfer velocity and hydraulic geometry in streams and small rivers. *Limnology & Oceanography*, *2*(1), 41–53. https://doi.org/10.1215/21573689-1597669

Read, J. S., Hamilton, D. P., Desai, A. R., Rose, K. C., MacIntyre, S., Lenters, J. D., et al. (2012). Lake-size dependency of wind shear and convection as controls on gas exchange. *Geophysical Research Letters*, *39*(9), L09405. https://doi.org/10.1029/2012GL051886

Regnier, P., Friedlingstein, P., Ciais, P., Mackenzie, F. T., Gruber, N., Janssens, I. A., et al. (2013). Anthropogenic perturbation of the carbon fluxes from land to ocean. *Nature Geoscience*, *6*(8), 597–607. https://doi.org/10.1038/ngeo1830

Regnier, P., Resplandy, L., Najjar, R. G., & Ciais, P. (2022). The land-to-ocean loops of the global carbon cycle. *Nature*, *603*(7901), 401–410. https://doi.org/10.1038/s41586-021-04339-9

Richey, J. E., Melack, J. M., Aufdenkampe, A. K., Ballester, V. M., & Hess, L. L. (2002). Outgassing from Amazonian rivers and wetlands as a large tropical source of atmospheric CO_2. *Nature*, *416*(6881), 617–620. https://doi.org/10.1038/416617a

Rocher-Ros, G., Sponseller, R. A., Lidberg, W., Mörth, C.-M., & Giesler, R. (2019). Landscape process domains drive patterns of CO_2 evasion from river networks. *Limnology and Oceanography Letters*, *4*, 87–95. https://doi.org/10.1002/lol2.10108

Roland, F. A. E., Darchambeau, F., Morana, C., & Borges, A. V. (2017). Nitrous oxide and methane seasonal variability in the epilimnion of a large tropical meromictic lake (Lake Kivu, East-Africa). *Aquatic Sciences*, *79*(2), 209–218. https://doi.org/10.1007/s00027-016-0491-2

Rosamond, M. S., Thuss, S. J., & Schiff, S. L. (2012). Dependence of riverine nitrous oxide emissions on dissolved oxygen levels. *Nature Geoscience*, *5*(10), 715–718. https://doi.org/10.1038/ngeo1556

Rosentreter, J. A., Borges, A. V., Deemer, B. R., Holgerson, M. A., Liu, S., Song, C., et al. (2021). Half of global methane emissions come from highly variable aquatic ecosystem sources. *Nature Geoscience*, *14*(4), 225–230. https://doi.org/10.1038/s41561-021-00715-2

Rovelli, L., Olde, L. A., Heppell, C. M., Binley, A., Yvon-Durocher, G., Glud, R. N., & Trimmer, M. (2022). Contrasting biophysical controls on carbon dioxide and methane outgassing from streams. *Journal of Geophysical Research: Biogeosciences*, *127*(1), e2021JG006328. https://doi.org/10.1029/2021JG006328

Sawakuchi, H. O., Martin, G., Peura, S., Bertilsson, S., Karlsson, J., & Bastviken, D. (2021). Phosphorus regulation of methane oxidation in water from ice-covered lakes. *Journal of Geophysical Research: Biogeosciences*, *126*(9), e2020JG006190. https://doi.org/10.1029/2020jg006190

Schilder, J., Bastviken, D., van Hardenbroek, M., Kankaala, P., Rinta, P., Stotter, T., & Heiri, O. (2013). Spatial heterogeneity and lake morphology affect diffusive greenhouse gas emission estimates of lakes. *Geophysical Research Letters*, *40*(21), 5752–5756. https://doi.org/10.1002/2013gl057669

Seitzinger, S. P., & Kroeze, C. (1998). Global distribution of nitrous oxide production and N inputs in freshwater and coastal marine ecosystems. *Global Biogeochemical Cycles*, *12*(1), 93–113. https://doi.org/10.1029/97GB03657

Seitzinger, S. P., Kroeze, C., & Styles, R. V. (2000). Global distribution of N_2O emissions from aquatic systems: Natural emissions and anthropogenic effects. *Atmospheric Nitrous Oxide*, *2*(3), 267–279. https://doi.org/10.1016/S1465-9972(00)00015-5

Sepulveda-Jauregui, A., Walter Anthony, K. M., Martinez-Cruz, K., Greene, S., & Thalasso, F. (2015). Methane and carbon dioxide emissions from 40 lakes along a North–South latitudinal transect in Alaska. *Biogeosciences*, *12*(11), 3197–3223. https://doi.org/10.5194/bg-12-3197-2015

Serikova, S., Pokrovsky, O. S., Laudon, H., Krickov, I. V., Lim, A. G., Manasypov, R. M., & Karlsson, J. (2019). High carbon emissions from thermokarst lakes of western Siberia. *Nature Communications*, *10*(1), 1552. https://doi.org/10.1038/s41467-019-09592-1

Shelley, F., Abdullahi, F., Grey, J., & Trimmer, M. (2015). Microbial methane cycling in the bed of a chalk river: Oxidation has the potential to match methanogenesis enhanced by warming. *Freshwater Biology*, *60*(1), 150–160. https://doi.org/10.1111/fwb.12480

Sieczko, A. K., Nguyen Thanh, D., Schenk, J., Gustav, P., David, R., Sawakuchi Henrique, O., & Bastviken, D. (2020). Diel variability of methane emissions from lakes. *Proceedings of the National Academy of Sciences of the United States of America*, *117*(35), 21488–21494. https://doi.org/10.1073/pnas.2006024117

Sobek, S., DelSontro, T., Wongfun, N., & Wehrli, B. (2012). Extreme organic carbon burial fuels intense methane bubbling in a temperate reservoir. *Geophysical Research Letters*, *39*(1), L01401. https://doi.org/10.1029/2011GL050144

Soued, C., del Giorgio, P. A., & Maranger, R. (2016). Nitrous oxide sinks and emissions in boreal aquatic networks in Québec. *Nature Geoscience*, *9*(2), 116–120. https://doi.org/10.1038/ngeo2611

Stanley, E. H., Casson, N. J., Christel, S. T., Crawford, J. T., Loken, L. C., & Oliver, S. K. (2016). The ecology of methane in streams and rivers: Patterns, controls, and global significance. *Ecological Monographs*, *86*(2), 146–171. https://doi.org/10.1890/15-1027

Stavert, A. R., Saunois, M., Canadell, J. G., Poulter, B., Jackson, R. B., Regnier, P., et al. (2022). Regional trends and drivers of the global methane budget. *Global Change Biology*, *28*(1), 182–200. https://doi.org/10.1111/gcb.15901

Stepanenko, V., Mammarella, I., Ojala, A., Miettinen, H., Lykosov, V., & Vesala, T. (2016). LAKE 2.0: A model for temperature, methane, carbon dioxide and oxygen dynamics in lakes. *Geoscientific Model Development*, *9*(5), 1977–2006. https://doi.org/10.5194/gmd-9-1977-2016

St. Louis, V. L., Kelly, C. A., Duchemin, É., Rudd, J. W. M., & Rosenberg, D. M. (2000). Reservoir surfaces as sources of greenhouse gases to the atmosphere: A global estimate: Reservoirs are sources of greenhouse gases to the atmosphere, and their surface areas have increased to the point where they should be included in global inventories of anthropogenic emissions of greenhouse gases. *BioScience*, *50*(9), 766–775. https://doi.org/10.1641/0006-3568(2000)050[0766:RSASOG]2.0.CO;2

Subin, Z. M., Riley, W. J., & Mironov, D. (2012). An improved lake model for climate simulations: Model structure, evaluation, and sensitivity analyses in CESM1. *Journal of Advances in Modeling Earth Systems*, *4*(1), M02001. https://doi.org/10.1029/2011MS000072

Tan, Z., & Zhuang, Q. (2015a). Methane emissions from pan-Arctic lakes during the 21st century: An analysis with process-based models of lake evolution and biogeochemistry. *Journal of Geophysical Research: Biogeosciences*, *120*(12), 2641–2653. https://doi.org/10.1002/2015JG003184

Tan, Z., & Zhuang, Q. (2015b). Arctic lakes are continuous methane sources to the atmosphere under warming conditions. *Environmental Research Letters*, *10*(5), 054016. https://doi.org/10.1088/1748-9326/10/5/054016

Telmer, K., & Veizer, J. (1999). Carbon fluxes, pCO_2 and substrate weathering in a large northern river basin, Canada: Carbon isotope perspectives. *Chemical Geology*, *159*(1), 61–86. https://doi.org/10.1016/S0009-2541(99)00034-0

Teodoru, C. R., Nyoni, F. C., Borges, A. V., Darchambeau, F., Nyambe, I., & Bouillon, S. (2015). Dynamics of greenhouse gases (CO_2, CH_4, N_2O) along the Zambezi River and major tributaries, and their importance in the riverine carbon budget. *Biogeosciences*, *12*(8), 2431–2453. https://doi.org/10.5194/bg-12-2431-2015

Tian, H., Ren, W., Yang, J., Tao, B., Cai, W., Lohrenz, S. E., et al. (2015). Climate extremes dominating seasonal and interannual variations in carbon export from the Mississippi River Basin. *Global Biogeochemical Cycles*, *29*(9), 1333–1347. https://doi.org/10.1002/2014GB005068

Tian, H., Yang, Q., Najjar, R. G., Ren, W., Friedrichs, M. A. M., Hopkinson, C. S., & Pan, S. (2015). Anthropogenic and climatic influences on carbon fluxes from eastern North America to the Atlantic Ocean: A process-based modeling study. *Journal of Geophysical Research: Biogeosciences*, *120*(4), 757–772. https://doi.org/10.1002/2014JG002760

Tonina, D., Marzadri, A., Bellin, A., Dee, M. M., Bernal, S., & Tank, J. L. (2021). Nitrous oxide emissions from drying streams and rivers. *Geophysical Research Letters*, *48*(24), e2021GL095305. https://doi.org/10.1029/2021GL095305

Tranvik, L. J., Downing, J. A., Cotner, J. B., Loiselle, S. A., Striegl, R. G., Ballatore, T. J., et al. (2009). Lakes and reservoirs as regulators of carbon cycling and climate. *Limnology & Oceanography*, *54*(6part2), 2298–2314. https://doi.org/10.4319/lo.2009.54.6_part_2.2298

Ulseth, A. J., Hall, R. O., Boix Canadell, M., Madinger, H. L., Niayifar, A., & Battin, T. J. (2019). Distinct air–water gas exchange regimes in low- and high-energy streams. *Nature Geoscience*, *12*(4), 259–263. https://doi.org/10.1038/s41561-019-0324-8

Vachon, D., & Prairie, Y. T. (2013). The ecosystem size and shape dependence of gas transfer velocity versus wind speed relationships in lakes. *Canadian Journal of Fisheries and Aquatic Sciences*, *70*(12), 1757–1764. https://doi.org/10.1139/cjfas-2013-0241

Varadharajan, C., Hermosillo, R., & Hemond, H. F. (2010). A low-cost automated trap to measure bubbling gas fluxes. *Limnology and Oceanography: Methods*, *8*, 363–375. https://doi.org/10.4319/lom.2010.8.363

Venkiteswaran, J. J., Rosamond, M. S., & Schiff, S. L. (2014). Nonlinear response of riverine N_2O fluxes to oxygen and temperature. *Environmental Science & Technology*, *48*(3), 1566–1573. https://doi.org/10.1021/es500069j

Verpoorter, C., Kutser, T., Seekell, D. A., & Tranvik, L. J. (2014). A global inventory of lakes based on high-resolution satellite imagery. *Geophysical Research Letters*, *41*(18), 6396–6402. https://doi.org/10.1002/2014GL060641

Vesala, T., Huotari, J., Rannik, Ü., Suni, T., Smolander, S., Sogachev, A., et al. (2006). Eddy covariance measurements of carbon exchange and latent and sensible heat fluxes over a boreal lake for a full open-water period. *Journal of Geophysical Research*, *111*(D11), D11101. https://doi.org/10.1029/2005JD006365

Waldo, S., Beaulieu, J. J., Barnett, W., Balz, D. A., Vanni, M. J., Williamson, T., & Walker, J. T. (2021). Temporal trends in methane emissions from a small eutrophic reservoir: The key role of a spring burst. *Biogeosciences*, *18*(19), 5291–5311. https://doi.org/10.5194/bg-18-5291-2021

Walter Anthony, K. M., & Anthony, P. (2013). Constraining spatial variability of methane ebullition seeps in thermokarst lakes using point process models. *Journal of Geophysical Research: Biogeosciences*, *118*(3), 1015–1034. https://doi.org/10.1002/jgrg.20087

Wang, J., Walter, B. A., Yao, F., Song, C., Ding, M., Maroof, A. S., et al. (2021). GeoDAR: Georeferenced global dam and reservoir dataset for bridging attributes and geolocations. *Earth System Science Data Discussions*, 1–52. https://doi.org/10.5194/essd-2021-58

Webb, J. R., Hayes, N. M., Simpson, G. L., Leavitt, P. R., Baulch, H. M., & Finlay, K. (2019). Widespread nitrous oxide undersaturation in farm waterbodies creates an unexpected greenhouse gas sink. *Proceedings of the National Academy of Sciences of the United States of America*, *116*(20), 9814–9819. https://doi.org/10.1073/pnas.1820389116

Weiss, R. F. (1970). The solubility of nitrogen, oxygen and argon in water and seawater. *Deep-Sea Research and Oceanographic Abstracts*, *17*(4), 721–735. https://doi.org/10.1016/0011-7471(70)90037-9

Wik, M., Crill, P. M., Bastviken, D., Danielsson, Å., & Norbäck, E. (2011). Bubbles trapped in arctic lake ice: Potential implications for methane emissions. *Journal of Geophysical Research*, *116*(G3), G03044. https://doi.org/10.1029/2011JG001761

Wik, M., Varner, R. K., Anthony, K. W., MacIntyre, S., & Bastviken, D. (2016). Climate-sensitive northern lakes and ponds are critical components of methane release. *Nature Geoscience*, *9*(2), 99–105. https://doi.org/10.1038/ngeo2578

Wilkinson, J., Maeck, A., Alshboul, Z., & Lorke, A. (2015). Continuous seasonal river ebullition measurements linked to sediment methane formation. *Environmental Science & Technology*, *49*(22), 14121–13129. https://doi.org/10.1021/acs.est.5b01525

Wit, F., Müller, D., Baum, A., Warneke, T., Pranowo, W. S., Müller, M., & Rixen, T. (2015). The impact of disturbed peatlands on river outgassing in Southeast Asia. *Nature Communications*, *6*(1), 10155. https://doi.org/10.1038/ncomms10155

Yamazaki, D., Ikeshima, D., Sosa, J., Bates, P. D., Allen, G. H., & Pavelsky, T. M. (2019). MERIT hydro: A high-resolution global hydrography map based on latest topography dataset. *Water Resources Research*, *55*(6), 5053–5073. https://doi.org/10.1029/2019WR024873

Yang, P., Huang, J. F., Yang, H., Penuelas, J., Tang, K. W., Lai, D. Y. F., et al. (2021). Diffusive CH_4 fluxes from aquaculture ponds using floating chambers and thin boundary layer equations. *Atmospheric Environment*, *253*, 118384. Article 118384. https://doi.org/10.1016/j.atmosenv.2021.118384

Yao, Y., Tian, H., Shi, H., Pan, S., Xu, R., Pan, N., & Canadell, J. G. (2020). Increased global nitrous oxide emissions from streams and rivers in the Anthropocene. *Nature Climate Change*, *10*(2), 138–142. https://doi.org/10.1038/s41558-019-0665-8

Yvon-Durocher, G., Allen, A. P., Bastviken, D., Conrad, R., Gudasz, C., St-Pierre, A., et al. (2014). Methane fluxes show consistent temperature dependence across microbial to ecosystem scales. *Nature*, *507*(7493), 488–491. https://doi.org/10.1038/nature13164

Zhou, Y., Xu, X., Song, K., Yeerken, S., Deng, M., Li, L., et al. (2021). Nonlinear pattern and algal dual-impact in N_2O emission with increasing trophic levels in shallow lakes. *Water Research*, *203*, 117489. https://doi.org/10.1016/j.watres.2021.117489

Zhu, D., Wu, Y., Wu, N., Chen, H., He, Y., Zhang, Y., et al. (2015). Nitrous oxide emission from infralittoral zone and pelagic zone in a shallow lake: Implications for whole lake flux estimation and lake restoration. *Ecological Engineering*, *82*, 368–375. https://doi.org/10.1016/j.ecoleng.2015.05.032

Zscheischler, J., Mahecha, M. D., Avitabile, V., Calle, L., Carvalhais, N., Ciais, P., et al. (2017). Reviews and syntheses: An empirical spatiotemporal description of the global surface-atmosphere carbon fluxes: Opportunities and data limitations. *Biogeosciences*, *14*(15), 3685–3703. https://doi.org/10.5194/bg-14-3685-2017